



Evidence of microbial activity in a uranium roll-front deposit: Unlocking their potential role as bioenhancers of the ore genesis



Fadwa Jroundi ^{a,*}, Cristina Povedano-Priego ^a, María Pinel-Cabello ^a, Michael Descostes ^{b,c}, Pierre Grizard ^b, Bayaarma Purevsan ^d, Mohamed L. Merroun ^a

^a Department of Microbiology, Faculty of Science, University of Granada, Avda. Fuentenueva s/n, 18071 Granada, Spain

^b ORANO Mining, 125 Avenue de Paris, 92330 Châtillon, France

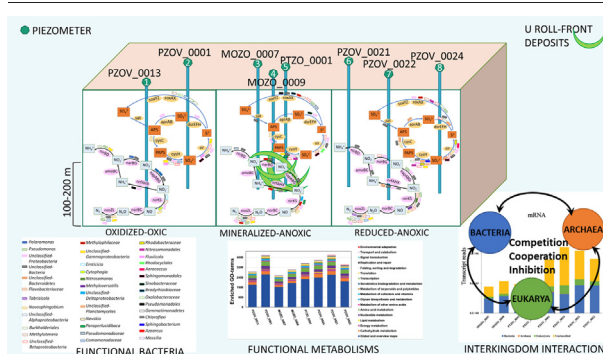
^c Centre de Géosciences, MINES ParisTech, PSL University, 35 rue St Honoré, 77300 Fontainebleau, France

^d Badrakh Energy LLC, Jamyang Gun Avenue - 9, Sukhbaatar district, 1st khoroo, UB-14240, Mongolia

HIGHLIGHTS

- Microbes involve mechanisms for the adaptation to U roll-front orebody environment.
- All domains of life, especially *Bacteria*, play a key role in biogeochemical cycling.
- Assimilation of N, S, and C is clue for bacterial resistance to extreme conditions.
- DNA repair, homeostasis, and metal tolerance genes are adopted to survive high stress.
- By their strong activities, microbes are involved in the roll-front orebody genesis.

GRAPHICAL ABSTRACT



ARTICLE INFO

Editor: Frederic Coulon

Keywords:
Roll-front deposit
Metatranscriptomes
Microbial metabolisms
Uranium
Ore genesis
ISR

ABSTRACT

Uranium (U) roll-front deposits constitute a valuable source for an economical extraction by *in situ* recovery (ISR) mining. Such technology may induce changes in the subsurface microbiota, raising questions about the way their activities could build a functional ecosystem in such extreme environments (i.e.: oligotrophy and high SO_4 concentration and salinity). Additionally, more information is needed to dissipate the doubts about the microbial role in the genesis of such U orebodies. A U roll-front deposit hosted in an aquifer driven system (in Zoovch Ovoo, Mongolia), intended for mining by acid ISR, was previously explored and showed to be governed by a complex bacterial diversity, linked to the redox zonation and the geochemical conditions. Here for the first time, transcriptional activities of microorganisms living in such U ore deposits are determined and their metabolic capabilities allocated in the three redox-inherited compartments, naturally defined by the roll-front system. Several genes encoding for crucial metabolic pathways demonstrated a strong biological role controlling the subsurface cycling of many elements including nitrate, sulfate, metals and radionuclides (e.g.: uranium), through oxidation-reduction reactions. Interestingly, the discovered transcriptional behaviour gives important insights into the good microbial adaptation to the geochemical conditions and their active contribution to the stabilization of the U ore deposits. Overall, evidences on the importance of these microbial metabolic activities in the aquifer system are discussed that may clarify the doubts on the microbial role in the genesis of low-temperature U roll-front deposits, along the Zoovch Ovoo mine.

* Corresponding author.
E-mail address: fadwa@ugr.es (F. Jroundi).

1. Introduction

Naturally occurring uranium (U) is one of the most important resources for dealing with the today increasing interest in the nuclear energy industry. Acid *in situ* recovery (ISR) has been extensively employed for U mining from low grade ores assimilated to roll-fronts (Ruiz et al., 2019; Seredkin et al., 2016; Zhao et al., 2018), providing more than a half of U production worldwide (IAEA and NEA, 2018). Uranium roll-front-type deposits occur as massive sub-tabular sandstone-hosted U minerals when oxidized fluids charged with dissolved elements, including organic carbon, flow through the system. The consequent mineralization results from the interaction of such oxidized fluids with reducing agents creating a uranium ore localized between oxidized and reduced sandstone (Akhtar et al., 2017; Bhattacharyya et al., 2017; Jin et al., 2020; Min et al., 2005). In the roll-front deposits, U(VI) reduction was usually attributed to abiotic reactions involving redox active minerals (pyrite and mackinawite), sulfide and sulfur species, as well as reactions of Fe(II) and thiols, as reduced organic functional groups, in low-temperature environments such as those of the Zoovch Ovoo deposits (Burns and Finch, 2018; Cumberland et al., 2016; Descostes et al., 2010; Granger and Warren, 1969; Grozeva et al., 2022; Li et al., 2015; Reynolds and Goldhaber, 1983; Wersin et al., 1994). The role of microbial activity in U ore genesis was, at first, thought to be limited to the providing of sulfides as a reducing agent as observed in the framboidal pyrites (Rallakis et al., 2021, 2019). However, later on, bacteria was proven to play a key role in U deposit formation by the generation of biogenic non-crystalline U(IV) as a major component of the U roll-front orebodies (Bhattacharyya et al., 2017). Such observation would indicate that the bacterial communities are able to adapt to specific geochemical conditions in environments related to U roll-front deposits.

ISR mining of such U ores is carried out through the injection of an acid leach solution (mainly sulfuric acid) directly in the orebody and pumping to the surface a pregnant solution for the further metal extraction at a processing facility (Seredkin et al., 2016). Although, it largely limits the environmental footprint resulting from other mining technologies (e.g.: waste-rocks, mining tailing), this strategy present an effect on the natural aquifer (bio)geochemistry through the variation of pH, potential increase in the mobility of metals and radionuclides and changes in the microbial community (Sapsford et al., 2017). All these conditions would generate in the microbial populations inhabiting such environments, different stresses related, among others, to pH, heavy metals, oxidation, and DNA damage. Thus, such changes would promote the activity of those capable to resist the low pH and those known mainly for their S, P, N, and C assimilation. Therefore, characterizing the native microbial composition and functionality before any ISR application is crucial to afford important information, not only into the potential of U removal, but also concerning the active microbial contribution to the optimization of the ISR process and the further long-term groundwater remediation, including alternative remediation solutions as bioremediation (Coral et al., 2022; Yabusaki, 2014).

A suitable bacterial community structure has been proposed as one of the challenges for the long-term groundwater remediation and stabilization of U ISR sites (Bhattacharyya et al., 2017; Coral et al., 2018; Jroundi et al., 2020). While previous works, based on next generation sequencing (NGS), provided valuable information about the significant association between the bacterial communities and the environmental parameters in uranium contaminated aquifers (Ayangbenro et al., 2018; He et al., 2018; Hemme et al., 2010; Jroundi et al., 2020; Macur et al., 2001; Mtimunya and Chirwa, 2019), some important concerns remain to be clarified. We previously reported a description of the bacterial communities in pristine groundwater surrounding a U roll-front deposit at Zoovch Ovoo (Mongolia), planned to be mined by ISR acid injection (Jroundi et al., 2020). At this site, the U deposit (the mineralized compartment) is confined inside an aquifer driven system, mineralized under low temperatures (<40 °C) (Rallakis et al., 2021). The whole system occurs within a redox barrier comprising an oxidizing part on the up-gradient side of the orebody (the oxidized compartment), and a reducing part enriched in sulfides and organic matter on the down-gradient side (the reduced compartment). The previous study

showed the presence of specific bacterial populations nitrate-reducing, sulfate-reducing, iron-reducing, iron-oxidizing, and U(VI)-reducing bacteria strongly correlated with sulfate, nitrate, iron, and metals, suggesting either the preference of environmental conditions specific to this site or complementary functions. Nevertheless, DNA based analysis provide no insights on the active microbial community, highlighting only the potential physiological characteristics that are dominant under the specified environmental conditions. Still little is known about whether the bacterial communities are effectively metabolically active in such conditions or whether their activities are related to the distinct redox-inherited aquifer compartments observed in the U roll-front deposits. Generally, bacteria can exist in environments where they are not metabolically active making it difficult to relate their mere presence to the geochemical functionality of the roll front. RNA based metatranscriptomics provide insights into the bacterial metabolic versatility and functioning in each aquifer compartment by defining their involvement in creating an ecologically functional ecosystem. Besides, it helps to clarify the role of microorganisms in the genesis of U roll front deposits under low temperatures.

While a large number of complex environmental metatranscriptomes have been reported over the last decades, most of them have mainly focused on soil, freshwater, and marine systems, but lesser on aquifer environments and none on U roll-front systems (Gura and Rogers, 2020; Jewell et al., 2016; Sharma et al., 2019; Vavourakis et al., 2019). To the best of our knowledge, here for the first time, the whole metatranscriptome of an aquifer with three defined redox compartments, localized at >100 m depth and bearing a U roll-front deposit, is explored to highlight the microbial metabolic activity and functionality in such systems. This detailed analysis would help to resolve important ongoing doubts about the microbial stability and adaptation to contaminants and elucidate significant functions, biogeochemical pathways and important processes involved in the genesis of the sandstone-hosted roll-front U deposits (Bhattacharyya et al., 2017; Bonnetti et al., 2017; Min et al., 2005).

The objective of this study was to give a transcriptional proof of the metabolic pathways and the important activities involved in the biogeochemical processes in an aquifer bearing a U roll-front deposit (Zoovch Ovoo, Mongolia). Determination of the different functional genes (based on RNA-Seq), as well as the composition and structure of the active microorganisms (not exclusively based on phylum but also on genus characterization to better assess activities of the relevant bacteria) were performed. The present work addressed the first metatranscriptomic analysis in this type of environments, highlighting how the groundwater microbial communities are involved in and adapted to harsh environmental changes, including those related to U ISR environments (Coral et al., 2018). In addition, we provide some key information related to 1) the microbial role and the biogeochemical mechanisms involved in the genesis of the sedimentary U ore deposit at low temperatures and 2) the relevance and capacity of the naturally occurring active microorganisms in the neutralization of the ISR acids. All these clues would constitute a baseline for an effective and accurate remediation strategy at the ISR sites.

2. Material and methods

2.1. Site description and sampling

The studied site is located at the Gobi Desert of Mongolia at Zoovch Ovoo in Sainshand region. This region of Mongolia is known, since 2015, by recoverable uranium resources intended to be mined by acidic ISR technique. The Zoovch Ovoo deposits are mineralized roll-front consisting of massive sub-tabular sandstone deposits hosting >55,000 tons of U (IAEA and NEA, 2018). Groundwater samples were sourced from ~100 to 200 m depth as described in Jroundi et al. (2020) (Fig. S1). One and a half liters of water from each sample were aseptically vacuum filtered, using sterilized, polycarbonate, hydrophilic Isopore™ membrane filters (Millipore), first through 0.45 µm and then 0.22 µm pore size filters. Three replicates of each water sample were performed. The obtained filters were then fixed with phenol (5 % v/v prepared in ethanol) and rapidly

stored at -80°C until their use (Fig. S2). Relevant water chemistry features are published elsewhere (Jroundi et al., 2020).

2.2. RNA extraction, amplification and cDNA synthesis

Total RNA was extracted from the filters (joining both pore-sized filters) of each replicate using RNeasy® PowerWater kit (QIAGEN GmbH, Germany) following the manufacturer's instructions summarized in the Supplementary material (SM) S1. The residual genomic DNA was removed using TURBO DNA-free kit (Ambion) and the RNA purified using RNeasy MinElute Cleanup kit (Qiagen). The RNA concentrations were determined using Qubit Fluorometer (Jiang et al., 2015) and stored at -80°C . Purified RNA samples were converted to cDNA using the Ovation® RNA-Seq System V2 (NuGEN, US) following the manufacturer's instructions summarized in the SM S1. The cDNA was purified using Agencourt AMPure XP beads (Beckman Coulter Genomics, Danvers, MA, USA) followed immediately by the SPIA Amplification (isothermal strand displacement amplification) while cDNA still bound to the dry beads. The amplified SPIA cDNA was purified using QIAGEN MinElute Reaction Cleanup Kit (QIAGEN GmbH, Germany). Finally, the cDNA concentrations were determined using Qubit Fluorometer (Jiang et al., 2015) and stored at -20°C .

The determination of functional genes was carried out at LGC Genomics (Berlin, Germany), by amplicon sequencing on the Illumina NextSeq 500 V2 platform.

2.3. Bioinformatics and statistical analyses

The obtained reads were pre-processed by removing barcodes and Illumina adapters, demultiplexing of all libraries for each sequencing lane using the Illumina bcl2fastq 1.8.4 software. Read-ends were clipped of sequencing adapter remnants (of low base quality) from all raw reads, so that reads with a final length < 20 bases were discarded. Quality trimming of adapter-clipped reads was performed by running Trimmomatic (Bolger et al., 2014) to obtain a minimum average (Phred quality score of 10) over a window of ten bases. All reads with final length < 20 bases were discarded. rRNA sequences were filtered using RiboPicker 0.4.3 (Schmieder et al., 2012) and digitally normalized groups were obtained. Gene expression estimation was carried out with RSEM 1.2.14 (Li and Dewey, 2011), using Trinity (version 2.3.2; Grabherr et al., 2011) for the assembly of the RNA-seq data, where all scaffolds larger than 200 bp were kept. Functional annotations of the genes were performed using InterProScan (version 5.19-58.0) and Gene Ontology (GO). Clustering of the annotated transcripts was carried out using Explicet software, as well as CateGORizer (Hu et al., 2008) and REVIGO (Supek et al., 2011). Rarefaction curves and Heatmap of the obtained transcripts were carried out using the VEGAN v2.4-6 package in R v. 3.4.3., and the heatmap.2 function in the R plots v2.11.0 package, respectively. In addition, transcripts obtained in all water sample (including three replicates of each) were analyzed based on the Simpson Similarity Index using PAST3 (v.3.18) software and the output was visualized with the Principal Coordinate Analysis (PCoA).

Table 1

Chemistry of the water samples collected from the Zoovch Ovoo mine in Mongolia. Oxidation-reduction potential (ORP) is expressed in mV/SHE. O_2 , NH_4 , NO_3^- , SO_4 and DOC are presented in mg/L, ^{226}Ra in mBq/L, and the other elements are expressed in $\mu\text{g/L}$.

Ox: oxidized waters, Min: mineralized water, Red: reduced waters

Samples	pH	ORP	O_2	NH_4	NO_3^-	SO_4	DOC	As	Mn	Mo	Se	Li	Si	Sr	Fe	U	^{226}Ra	Ba
PZOV_0013 (Ox)	7.67	379.1	6.73	0.03	7.49	721	2.22	6.2	5	8.4	37	143	4600	2250	5	50	81	6.4
PZOV_0001 (Ox)	7.76	354.6	3.81	0.05	14.87	580	2.81	5.0	5	7.7	56	108	4840	2090	5	25	54	6.3
MOZO_0007 (Min)	7.71	172.3	0.01	0.02	1.10	682	3.67	5.0	117	17.0	118	154	5510	1240	15	1010	1731	16.0
MOZO_0009 (Min)	7.69	166.2	0.01	0.04	5.37	620	3.36	5.0	93	17.0	101	129	5740	1260	18	948	1834	14.0
PTZO_0001 (Min)	7.6	69.9	0.01	0.03	1.02	576	2.40	6.4	120	11.0	10	126	5480	875	142	644	3999	7.3
PZOV_0024 (Red)	8.15	-9.4	0.01	0.60	1.02	1235	3.53	14.0	218	53.0	10	177	4230	412	13	18	65	8.9
PZOV_0021 (Red)	8.16	3.8	0.01	0.49	1.02	823	2.73	5.0	36	25.0	10	136	4430	200	14	38	193	9.0
PZOV_0022 (Red)	8.17	-14.0	0.01	0.54	1.02	894	3.04	12.0	57	45.0	10	143	4250	194	26	2.3	102	8.4

2.4. Taxonomic characterization of active microorganisms

Phylogenetic identification of SSU rRNA scaffolds was carried out with Galaxy tools (usegalaxy.org). Obtained reads (Forward and Reverse) of each replicate/sample were at first assembled using pRESTO AssemblePairs toolkit (Vander Heiden et al., 2014). The assembled raw reads were annotated using kraken to assign taxonomic labels for active microbial diversity (Wood and Salzberg, 2014). Reconstructed SSU sequences abundances were calculated by SSU reads mapping back on SSU sequences with kraken-translate, which convert taxonomy IDs to names, and then with kraken-mpa-report tool a classification report for multiple samples was obtained (Lu and Salzberg, 2020).

Taxonomic assignments of mRNA transcripts were performed with the Contig Annotation tool (CAT) (Cambuy et al., 2016) using a local CAT database on July 2019, including gene calling, mapping of predicted open reading frames (ORFs) against the protein sequences from prokaryotes and microbial eukaryotes (nr protein database), and classification of the entire contig based on the individual ORFs available at the Galaxy webpage. Then, the counts were aggregated according to the assigned GO annotation and the enrichment analysis carried out at ShinyGO webpage (Ge et al., 2020) to underly molecular pathways and functional categories such as gene ontology (GO) and KEGG (Kyoto Encyclopedia of Genes and Genomes) databases.

2.5. Availability of data and material

The data of the Metatranscriptomes sequencing are accessible in the NCBI BioProject under the ID number PRJNA698761.

3. Results

3.1. Hydrochemistry and U roll-front structure

The different water samples sequenced here were geochemically characterized in a previous study (Jroundi et al., 2020) and showed to have a natural redox zonation related to the U roll-front deposit (Table 1). The samples PZOV_0001 and PZOV_0013, being the oxidized waters, were the only oxygenated samples (6.73 and 3.81 mg/L), with oxidation-reduction potential (ORP) values reaching 379.1 mV/SHE, and the highest NO_3^- values ranging from 7.49 to 14.87 mg/L. Samples MOZO_0007, MOZO_0009, and PTZO_0001 were the anoxic mineralized samples containing the U ore body with ORP values varying between +69.9 and +172.3 mV/SHE, and NO_3^- values ranging from 1.02 to 5.37 mg/L. Finally, the samples PZOV_0021, PZOV_0022, and PZOV_0024 were the anoxic reduced waters with ORP values of -9.4, 3.8 and -14 mV/SHE, respectively, and very low NO_3^- values (1.02 mg/L). In general, the water chemistry followed a redox dependent zonation through the roll-front system, where As, Mo and NH_4^+ showed higher concentrations in the reduced water samples, while Se, Fe, and Mn were present with higher concentrations in the ore area, along with U, Ba, and ^{226}Ra (Jroundi et al., 2020). In addition, in the studied water samples, U speciation is thought to be U

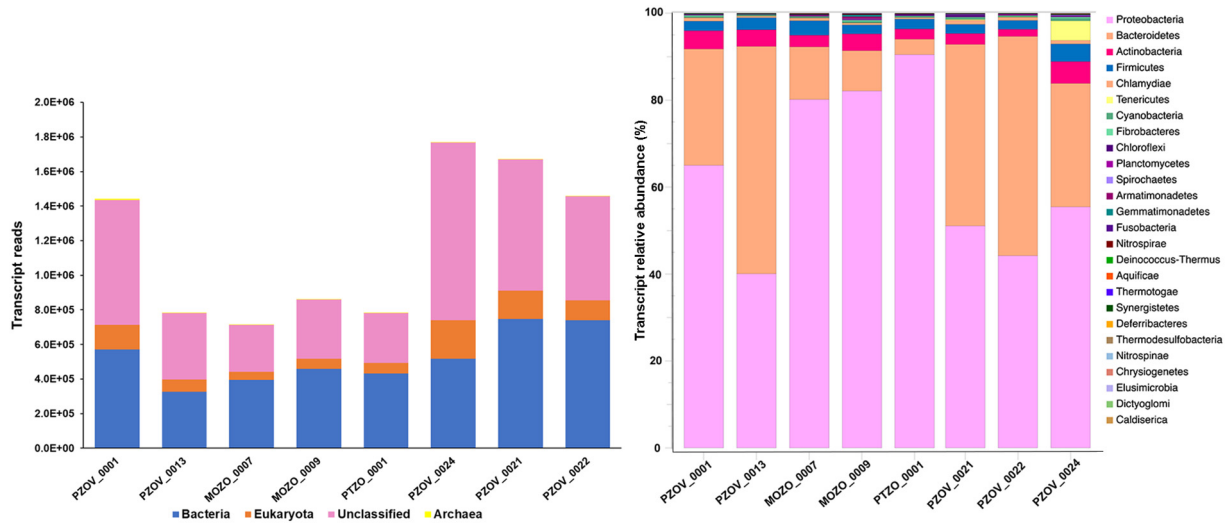


Fig. 1. Metatranscriptome data obtained from the active microbial communities of the oxidized, mineralized and reduced water samples. (A) mRNA reads distribution of the domains of life expressed in the different water samples. (B) Total prokaryotic community at phylum level based on the active mRNA transcripts.

(VI) as U(IV) is very insoluble (Reiller and Descostes, 2020). This assumption is in agreement with the water composition and the ORP and pH values of all samples explored in this study and showed in Table 1. Typical examples including groundwaters in such geochemical conditions are reported also in Reiller and Descostes (2020).

3.2. Active community members and functional gene diversity

Phylogenetic placement of *de novo* assembled mRNA transcripts from the water data collections showed that the three domains of life *Bacteria*, *Archaea*, and *Eukaryota* were obtained in the eight water samples collected from the three redox compartments (oxidized, mineralized, and reduced). However, *Bacteria* showed a clear dominance over *Archaea* and *Eukaryota* (Fig. 1).

Rarefaction curves of all samples' transcripts reached a plateau (Fig. S3), meaning that the sequencing was deep enough to detect major transcripts in the libraries. PCoA analysis revealed significant clustering of transcripts by water sample type (Fig. 2), where the oxidized oxic samples (PZOV_0013 and PZOV_0001) seem to be dominated by a different functional gene expression and/or richness compared to the other anoxic (mineralized and reduced) water samples. This same clustering has been also observed when the bacterial diversity of these water samples was previously studied in Jroundi et al. (2020).

The results are therefore presented here according to the redox zonation. Fig. 3 shows both phyla and genera annotated with the GO database, allowing the deciphering of the transcriptional activity in the different water samples (oxidized, mineralized and reduced water compartments). Only representatives of the dominant genera are presented here.

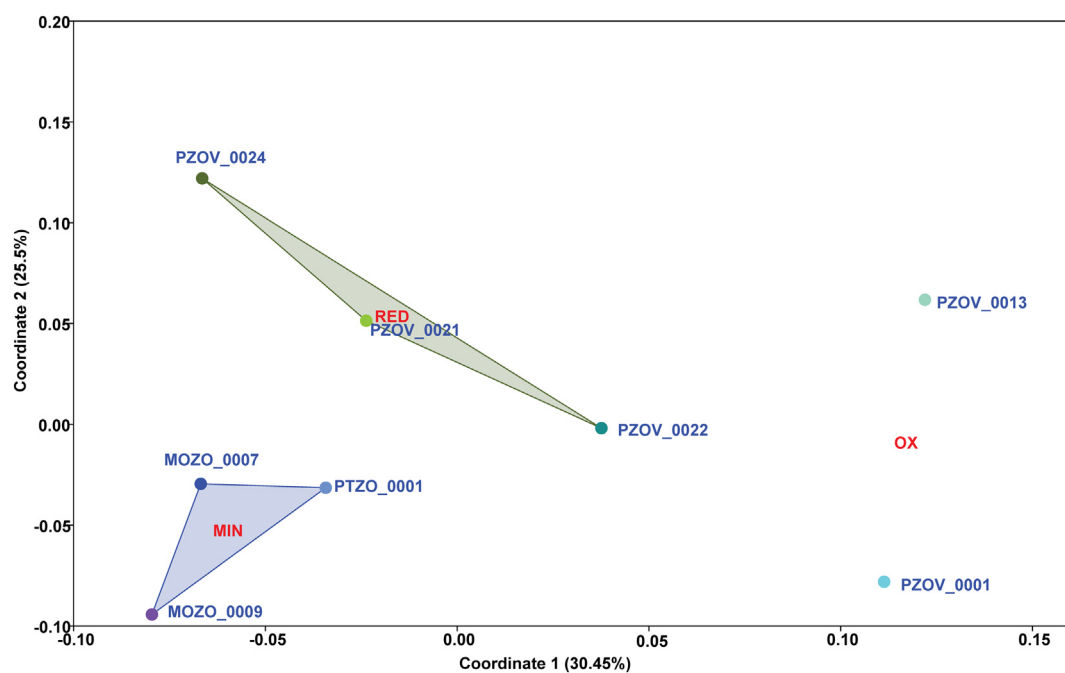


Fig. 2. PCoA of all studied water samples based on Simpson Similarity Index. PZOV_0013 and PZOV_0001: oxidized samples (upstream compartment); MOZO_0007, MOZO_0009 and PTZO_0001: Mineralized water samples (roll-front ore compartment); PZOV_0024, PZOV_0021, and PZOV_0022: reduced water samples (downstream compartment).

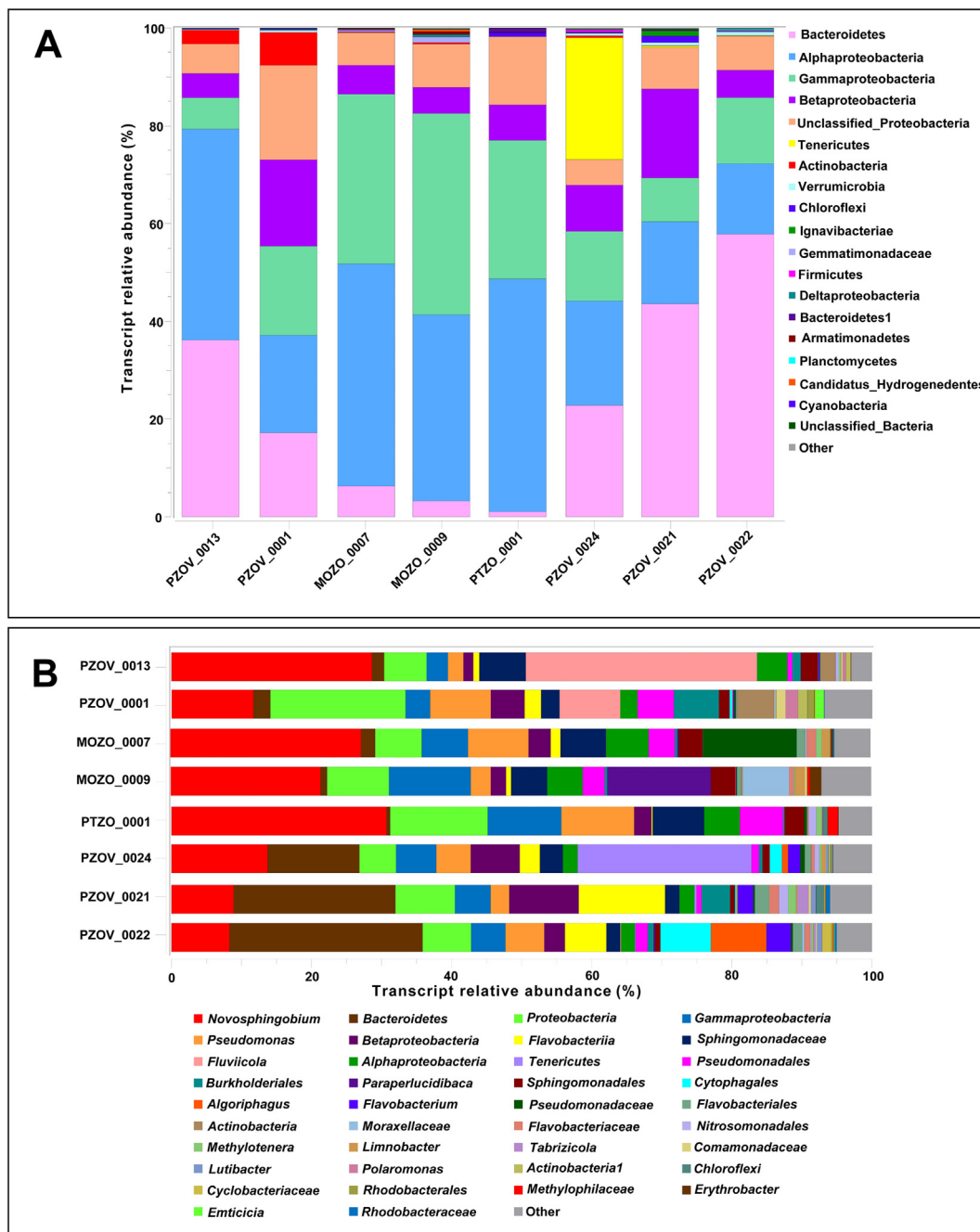


Fig. 3. Distribution of mRNA transcripts percentages of the taxonomical groups at phylum/class and genus level in the oxidized, mineralized and reduced water samples. (A) At phylum/class level classification. (B) At genus level classification.

3.2.1. Oxidized waters

Transcriptional activity in the oxidized water samples (PZOV_0001 and PZOV_0013) was assigned to classified *Bacteria* dominated by *Alphaproteobacteria* [199,399 and 431,318 TPM (transcript per million)] mainly aligned with *Novosphingobium* and unclassified-*Sphingomonadaceae*, followed by *Betaproteobacteria* (177,136 and 49,655 TPM) related to *Polaromonas* and unclassified-*Comamonadaceae* and *Burkholderiales*, *Gammaproteobacteria* (182,030 and 63,917 TPM) related to many *Pseudomonas* species (*P. stutzeri*, *P. fulva*, *P. mendocina*, *P. aeruginosa*, *P. fluorescens*) and unclassified-*Pseudomonadales*, and unclassified-*Proteobacteria* (193,025 and 60,684 TPM). Other mRNA transcripts were associated to *Bacteroidetes* (172,140 and 361,971 TPM) mainly aligned with *Fluviicola* and *Emticia*. In addition, many transcripts were related to unclassified members of

Actinobacteria (66,925 and 28,293 TPM), along with *Verrucomicrobia* (4302 and 1395 TPM), *Deltaproteobacteria* (1468 and 85 TPM), *Cyanobacteria* (1332 and 1162 TPM), *Firmicutes* (785 and 275 TPM), and *Planctomycetes* (455 and 380 TPM). To a lesser degree, other rare phyla were represented by *Deinococcus-Thermus* (91 and 317 TPM), *Choloroflexi* (91 and 63 TPM), *Ignavibacteriae* (46 and 0 TPM), *Oligoflexia* (46 and 232 TPM), and *Nitrospirae* (34 and 0 TPM). The *Archaea* lineages were represented by unclassified-*Archaea* (994,023, and 988,506 TPM), followed by *Euryarchaeota* (3396 and 0 TPM) and *Thaumarchaeota* (2581 and 11,494 TPM).

The composition of these transcriptionally active genera detected in the oxidized water samples was highly similar to that of the bacterial community obtained previously using the 16S rRNA genes sequencing analysis

(Jroundi et al., 2020). Some of the dominant genera, such as *Pseudomonas*, *Fluviicola*, *Burkholderia*, and *Novosphingobium*, showed a higher transcriptional activity (in mRNA) in comparison to the representatives detected in the previous 16S rRNA genes analysis, while *Polaromonas* and *Flavobacterium* showed a lower transcriptional activity than abundance (Supplementary data S1), with a relative abundance of 9.2 and 31.8 % (for *Polaromonas*) and of 2.4 and 4.2 % (for *Flavobacterium*) in PZOV_0001 and PZOV_0013, respectively.

3.2.2. Mineralized waters

In the mineralized water samples (MOZO_0007, MOZO_0009, and PTZO_0001) (Fig. 3), *Bacteria* lineages were dominated by *Alphaproteobacteria* (454,448, 381,467, and 476,469 TPM) aligned with *Novosphingobium*, unclassified-*Sphingomonadaceae*, *Erythrobacter*, *Sphingobium* and *Sphingomonas*, followed by *Gammaproteobacteria* (346,889, 411,501 and 283,113 TPM) mainly related to many *Pseudomonas* species, *Paraperlucidiabaca*, unclassified-*Moraxellaceae* and *Nevskia*, as well as *Betaproteobacteria* (59,504, 53,294, and 72,782 TPM) mainly aligned with *Limnobacter* and unclassified-*Methylphilaceae* and *-Nitrosomonadales*, as well as unclassified-*Deltaproteobacteria* (1129, 4546, and 1521 TPM), and unclassified members of *Proteobacteria* (66,624, 88,351, and 10,389 TPM). *Bacteroidetes* (62,992, 32,185 and 18,192 TPM) were also represented mainly by unclassified members and some aligned with unclassified members of *Flavobacteriaceae*, *Gemmatimonadetes* (2750, 11,488, and 46 TPM), along with *Firmicutes* (1744, 283, and 395 TPM), *Armatimonadetes* (1703, 5850, and 152 TPM), *Actinobacteria* (862, 3258, and 183 TPM), and some less-represented phyla. The *Archaea* lineages were represented by unclassified-*Archaea* (1,000,000, 903,846, and 90,909 TPM) and *Euryarchaeota* (0, 96,154, and 909,091 TPM) (Fig. 3).

Like for the oxidized water samples, the composition of the microbial population detected transcriptionally (this study) and by the previous 16S rRNA genes sequencing (Jroundi et al., 2020) was similar (Supplementary data S1), although the genera *Pseudomonas*, *Methylotenera*, *Limnobacter*, among others, showed an increase in their transcriptional activity in comparison to their relative abundance. Surprisingly, some genera were greatly under-detected using the 16S rRNA sequencing (Jroundi et al., 2020). For example, no *Novosphingobium* representatives were detected in the samples MOZO_0007 and MOZO_0009 by the previous 16S rRNA genes sequencing, while in this study it was one of the most transcriptionally abundant genus in the three mineralized samples (MOZO_0007, MOZO_0009, and PTZO_0001) with a relative abundance of 5.7, 7.4, and 7.7 %, respectively.

3.2.3. Reduced waters

More diverse *Bacteria* lineages were assigned to the mRNA transcripts obtained from the reduced water samples (PZOV_0021, PZOV_0022, and PZOV_0024) (Fig. 3). These included as dominant the phylum *Bacteroidetes* (437,230, 578,666, and 228,260 TPM) mainly aligned with *Flavobacterium*, *Lutibacter*, *Algoriphagus* and unclassified members of *Cytophagales* and *Cyclobacteriaceae*. Members of *Alphaproteobacteria* (168,069, 144,311, and 213,651 TPM) were represented by *Novosphingobium*, *Sphingomonadaceae*, and *Tabrizicola*, while *Betaproteobacteria* (181,969, 56,196, and 94,504 TPM) aligned with *Burkholderiales*, *Nitrosomonadales*, *Methylotenera*, and *Hydrogenophaga*. *Gammaproteobacteria* (89,291, 134,619, and 142,429 TPM) were related mainly to many *Pseudomonas* species. Also detected in these samples were unclassified-*Proteobacteria* (85,058, 69,383, and 52,371 TPM), *Chloroflexi* (13,273, 47, and 1228 TPM) aligned with unclassified members and *Anaerolineaceae*, *Ignavibacteriae* (10,582, 196, and 585 TPM), *Verrucomicrobia* (6062, 7187, and 5060 TPM) mainly related to *Opiritaceae*, *Tenericutes* (3101, 997, and 248,837 TPM), *Firmicutes* (749, 1948, and 4665 TPM), *Actinobacteria* (749, 511, 3978 TPM), along with *Deltaproteobacteria* (409, 1225, and 1345 TPM), *Planctomycetes* (409, 2718, and 102 TPM), and *Cyanobacteria* (192, 503, and 307 TPM). Rare phyla were also present in these waters including *Chlamydiae* (139, 16, and 234 TPM), *Chlorobi* (122, 314, and 15 TPM), *Calditrichaeota* (44, 16, and 146 TPM), *Acidobacteria* (35, 55, and 497 TPM), *Zetaproteobacteria* (35, 157, and 29 TPM), *Elusimicrobia* (26, 0, and 175 TPM), *Nitrospirinae*

(26, 24, and 0 TPM), and *Nitrospirae* (17, 346, and 132 TPM). The *Archaea* lineages were represented by unclassified-*Archaea* (993,846, 995,562, and 993,051 TPM), *Euryarchaeota* (6154, 3994, and 5272 TPM), *Thaumarchaeota* (0, 178, and 0 TPM), *Candidatus Thorarchaeota* (0, 0, and 1677 TPM), and *Candidatus Lokiarchaeota* (0, 266, and 0 TPM) (Fig. 3).

The top ten most transcriptionally active genera in these water samples were also detected in the previous 16S rRNA sequencing analysis as abundant genera, and in general the overall composition of the microbial population was very similar, with some exceptions (Supplementary data S1). For example, very low or no representatives of *Novosphingobium* and *Burkholderia* were detected by the 16S rRNA amplification, while their transcriptional activity in these reduced water samples was considerably high. The opposite occurs with *Hydrogenophaga* and *Rhodobacter*, which showed a high relative abundance (Jroundi et al., 2020), but a reduced transcriptional activity.

3.3. Metabolic processes in the aquifers surrounding the uranium roll-front deposits

Based on mRNA gene ontologies, the studied water microbial communities were enriched by transcripts encoding for several different functional categories (Fig. 4). These consisted of many pathways implicated in the Metabolism, Cellular Processing, Organismal Systems, Genetic Information processing, and Environmental Information Processing. Within the Global and overview maps of the Metabolism, the water microbial communities were particularly active in pathways such as “Metabolic pathways”, “Carbon metabolism”, “Biosynthesis of amino acids”, “Biosynthesis of secondary metabolites”, “Microbial metabolism in diverse environments”, and “Fatty acid metabolism”. Results are also here presented according to the redox zonation. The microbial activity is expressed by a diverse community, which increase from the oxidized to the reduced compartments.

3.3.1. Microbial activity in the oxidized waters

A total of 63 and 60 functional categories were identified in the oxidized water samples (PZOV_0001 and PZOV_0013) (Figs. 5 and S4). These were dominated by transcripts encoding for many pathways in the Metabolism, where in addition to the global overview metabolism mentioned above, they were involved in all functional classes and, all of which, except for the Tricarboxylic Acid cycle (TCA), were upregulated in PZOV_0001 water sample. The metabolic pathways involved within the TCA cycle with 22 and 26 GO-terms were attributed to the *Alphaproteobacteria* and unknown-organisms in PZOV_0013 and to the *Betaproteobacteria*, *Bacteroidetes*, and unclassified-*Proteobacteria* in PZOV_0001. The “Energy metabolism” included Oxidative phosphorylation that was attributed to *Proteobacteria* (*Beta* and *Gamma*), *Bacteroidetes*, *Actinobacteria*, unclassified-*Bacteria*, *Eukaryota* (mainly *Ascomycota*) and unknown-organisms in PZOV_0013, and in PZOV_0001 to all of them in addition to *Archaea*, and *Bacillariophyta* form the *Eukaryota*. Pathways involved in the Sulfur metabolism were identified with 33 and 23 GO-terms in these oxidized water samples, and the transcripts were attributed to *Proteobacteria* (*Alpha*, and unclassified), *Bacteroidetes*, unclassified-*Bacteria* in both samples, additionally to *Bacillariophyta*, and unknown-organisms in PZOV_0001 and *Actinobacteria* in PZOV_0013. Nitrogen metabolism was expressed by 10 and 11 GO-terms attributed mainly to *Gammaproteobacteria*, *Actinobacteria* and unclassified-*Eukaryota* in PZOV_0001 and to *Proteobacteria* (*Beta*, and unclassified), *Actinobacteria* and unclassified-*Eukaryota* in PZOV_0013. Both purine and pyrimidine metabolisms from the “Nucleotide metabolism” were particularly enriched in these water samples. mRNA transcripts were identified for Genetic Information Processing, including actual translation (the pathways Aminoacyl-tRNA biosynthesis assigned to all active Prokaryotes classified here with the exception of *Actinobacteria*, beside *Eukaryota* and unknown-organisms), RNA degradation, Replication and repair (mainly by the Homologous recombination).

3.3.2. Microbial activity in the mineralized waters

In the mineralized samples (MOZO_0007, MOZO_0009, and PTZO_0001), the bacterial metabolic activity was functionally classified in

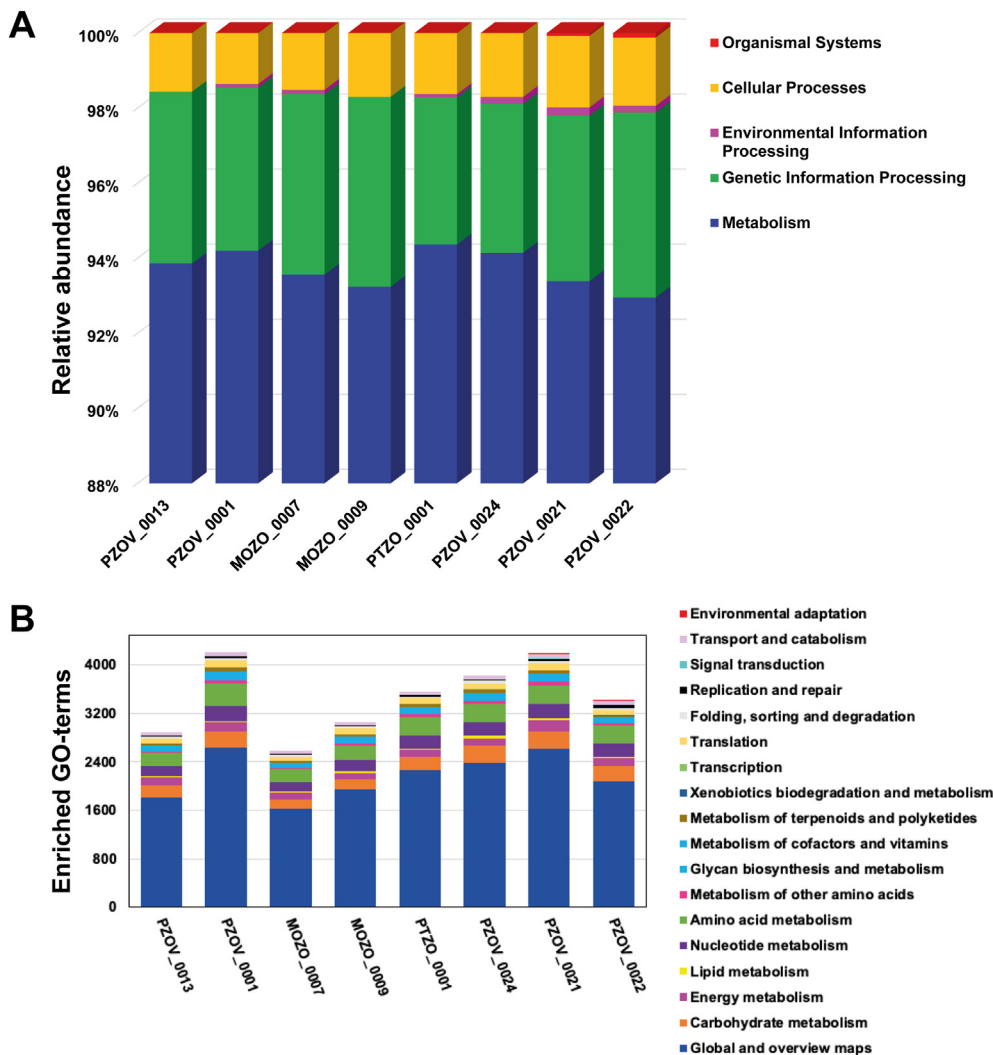


Fig. 4. Percent relative abundance distribution of transcripts assigned to dominant KEGG pathways and the enriched GO terms distribution on the major levels in the studied water samples. A) First level KEGG pathways. B) Second level KEGG pathways.

59, 64, and 62 functional categories, respectively (Figs. 6 and S5). Comparisons of the global maps in the Metabolism of these water samples indicated a more active PTZO_0001 microbial community in Metabolic pathways, Carbon metabolism, Biosynthesis of secondary metabolites, Microbial metabolism in diverse environments, Biosynthesis of amino acids and 2-Oxocarboxylic acid metabolism.

Here, the metabolic pathways involved in the TCA cycle (with 17, 7, and 14 GO-terms, respectively) were attributed to the *Gammaproteobacteria*, unclassified-*Bacteria*, unclassified-*Eukaryota* and unknown-organisms in MOZO_0007, to the unclassified-*Bacteria* in MOZO_0009, and to the *Betaproteobacteria*, unclassified-*Eukaryota*, and unknown-organisms in PTZO_0001. The “Energy metabolism” included Oxidative phosphorylation which was attributed to *Proteobacteria* (*Beta*, and unclassified), *Bacteroidetes*, unclassified-*Bacteria*, unclassified-*Eukaryota* and unknown-organisms in MOZO_0007 (45 GO-terms) and in PTZO_0001 (except for the unclassified-*Bacteria*, 33 GO-terms), and to the *Proteobacteria* (*Beta*, and unclassified), *Bacteroidetes*, *Actinobacteria*, *Armatimonadetes*, *Gemmatimonadetes*, unclassified-*Bacteria*, *Eukaryota* (*Ascomycota*) and unknown-organisms in MOZO_0009 (54 GO-terms). Pathways for the “Carbon fixation in photosynthetic organisms” were identified with 22, 17, and 29 GO-terms, respectively, and assigned to the *Alphaproteobacteria*, and unclassified-*Bacteria*, in addition to unknown-organisms in MOZO_0007 and also to *Gammaproteobacteria* in PTZO_0001. This reference pathway also includes “Carbon fixation by

prokaryotes”, using the “Reductive citrate cycle (rTCA)”, “Wood-Ljungdahl pathway”, and “Phosphate acetyltransferase-acetate kinase pathway”, among some others, for the autotrophic carbon fixation. It is well known that in aphotic environments, carbon fixation could be mediated by rTCA cycle in a process called “dark primary reduction”. This pathway plays a major role in the primary production in oceanic and subsurface environments (Overholt et al., 2022). The use of the reductive TCA cycle was also confirmed in a variety of strict anaerobic or microaerobic bacteria and anaerobic archaea (Hügler et al., 2005, 2007).

Here, pathways involved in the Sulfur metabolism were identified with 19, 22, and 35 GO-terms, and the transcripts were attributed to *Proteobacteria* (*Alpha*, and *Gamma*), *Bacteroidetes*, and unclassified-*Bacteria* in MOZO_0007, to *Proteobacteria* (*Alpha*, *Beta*, and *Gamma*), *Ascomycota* and unknown-organisms in MOZO_0009, and to *Proteobacteria* (*Alpha*, *Gamma*, and unclassified), *Bacteroidetes*, *Ascomycota*, unclassified-*Bacteria*, and unknown-organisms in PTZO_0001. Nitrogen metabolism was expressed by 16, 12 and 15 GO-terms attributed mainly to *Bacteroidetes* and unclassified-*Bacteria*, in addition to *Gammaproteobacteria* and unknown-organisms in MOZO_0007, to *Gammaproteobacteria* in MOZO_0009, and to unclassified-*Proteobacteria* and unknown-organisms in PTZO_0001. Both purine and pyrimidine metabolisms from the “Nucleotide metabolism” were expressed in these water samples and particularly enriched in the PTZO_0001 water sample. mRNA transcripts were identified for Genetic Information Processing, including

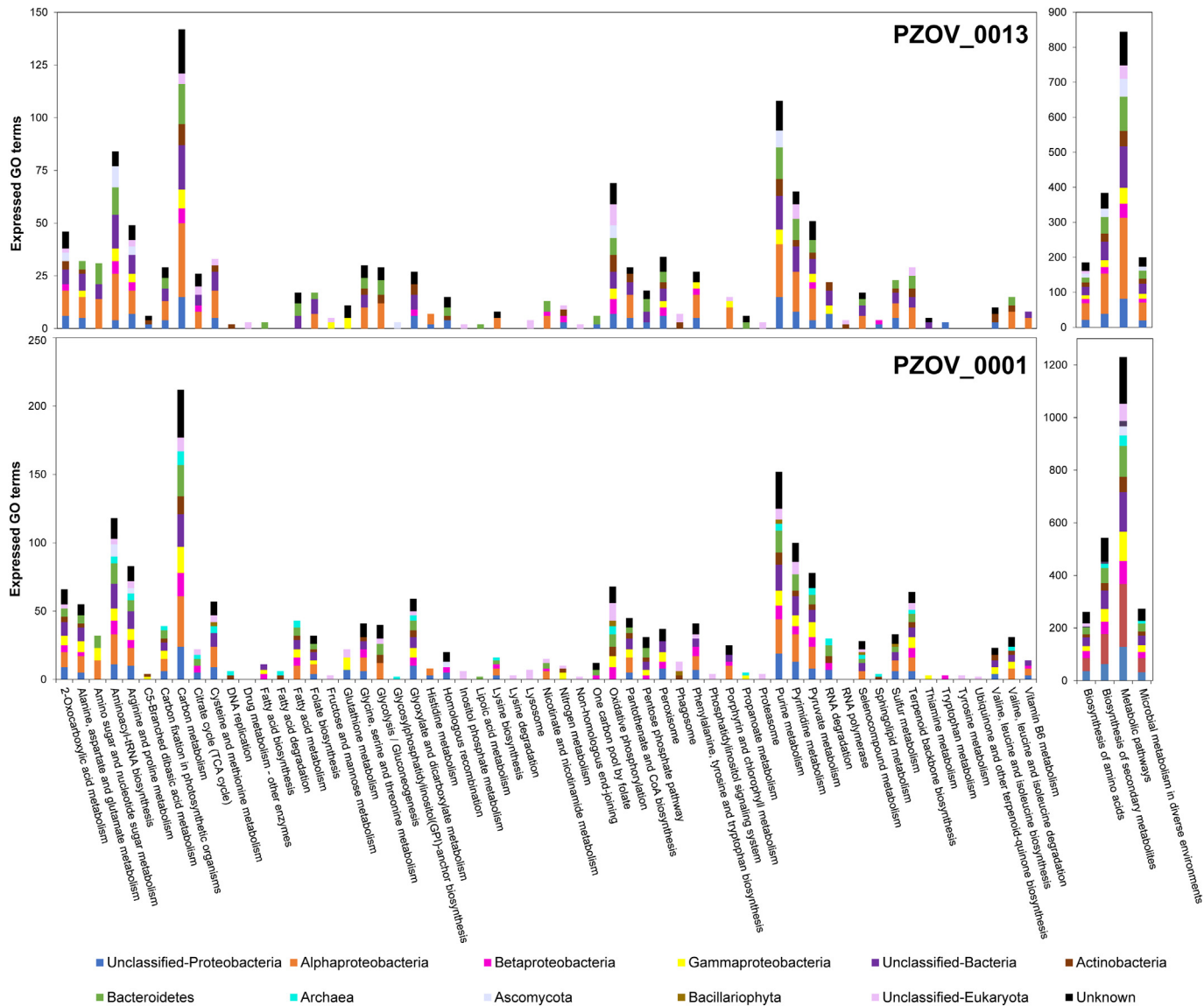


Fig. 5. Gene expression profile in the oxidized water samples. Transcripts annotated with Gene Ontology (GO) “Biological Process” terms and enriched to KEGG database are shown. GO processes assigned to a phylum (or other taxonomical classification) of <1 % of the total were integrated as *Bacteria*, *Archaea*, or *Eukarya*.

transcription (the pathway RNA polymerase attributed to *Actinobacteria* in MOZO_0009), actual translation [the pathways Aminoacyl-tRNA biosynthesis (70, 82, and 91 GO-terms) assigned in all three samples to all active Prokaryotes classified here with the exception of *Actinobacteria* in MOZO_0009, beside *Eukaryota* and unknown-organisms], Ribosome biogenesis [in eukaryotes (assigned to *Ascomycota*), in *Actinobacteria*, and in *Chloroflexi*], and mRNA surveillance pathway (*Ascomycota* and unclassified-*Eukaryota*). Pathways for RNA degradation (24, 18, and 14 GO-terms) attributed to unclassified-*Bacteria*, -*Eukaryota*, unknown-organisms and *Gammaproteobacteria*, *Betaproteobacteria* or *Chloroflexi* were detected in all mineralized water samples. In addition, some transcripts encoding pathways for Protein export, Ubiquitin mediated proteolysis, and Proteasome were also slightly expressed here. Replication and repair were mainly represented by pathways for DNA replication, Nucleotide excision repair and Homologous recombination.

3.3.3. Microbial activity in the reduced water

A high proportion of mRNA transcripts were identified in the communities of the reduced samples (PZOV_0024, PZOV_0021, and PZOV_0022), which were classified in 64, 64, and 67 functional categories, respectively

(Figs. 7 and S6). As with the previous samples, the microbial communities of these reduced samples were characterized by a more active metabolic global maps in PZOV_0021 including many transcripts encoding for Metabolic pathways, Carbon metabolism, Microbial metabolism in diverse environments, 2-Oxocarboxylic acid metabolism, Biosynthesis of secondary metabolites, and Biosynthesis of amino acids, with the exception of Fatty acid metabolism, which was more enriched in PZOV_0024 than in the others.

The metabolic pathways involved in the TCA cycle were expressed in these reduced waters more than in all the others studied here, with 30, 40, and 23 GO-terms enriched in PZOV_0024, PZOV_0021, and PZOV_0022, respectively. These pathways for the TCA cycle were attributed to *Proteobacteria* (*Alpha*, and *Beta*), unclassified-*Bacteria*, unclassified-*Eukaryota* and unknown-organisms in PZOV_0024, all of these beside *Bacteroidetes* and *Archaea* in PZOV_0021, and to *Proteobacteria* (*Beta*, and unclassified), *Archaea*, unclassified-*Eukaryota*, and unknown-organisms in PZOV_0022. The “Energy metabolism” included Oxidative phosphorylation (48, 86, and 65 GO-terms), which was attributed to *Proteobacteria* (*Beta*, and unclassified), *Verrumicrobia*, unclassified-*Bacteria*, *Archaea*, and unclassified-*Eukaryota* in PZOV_0024, to *Proteobacteria* (*Beta*, *Gamma*, and

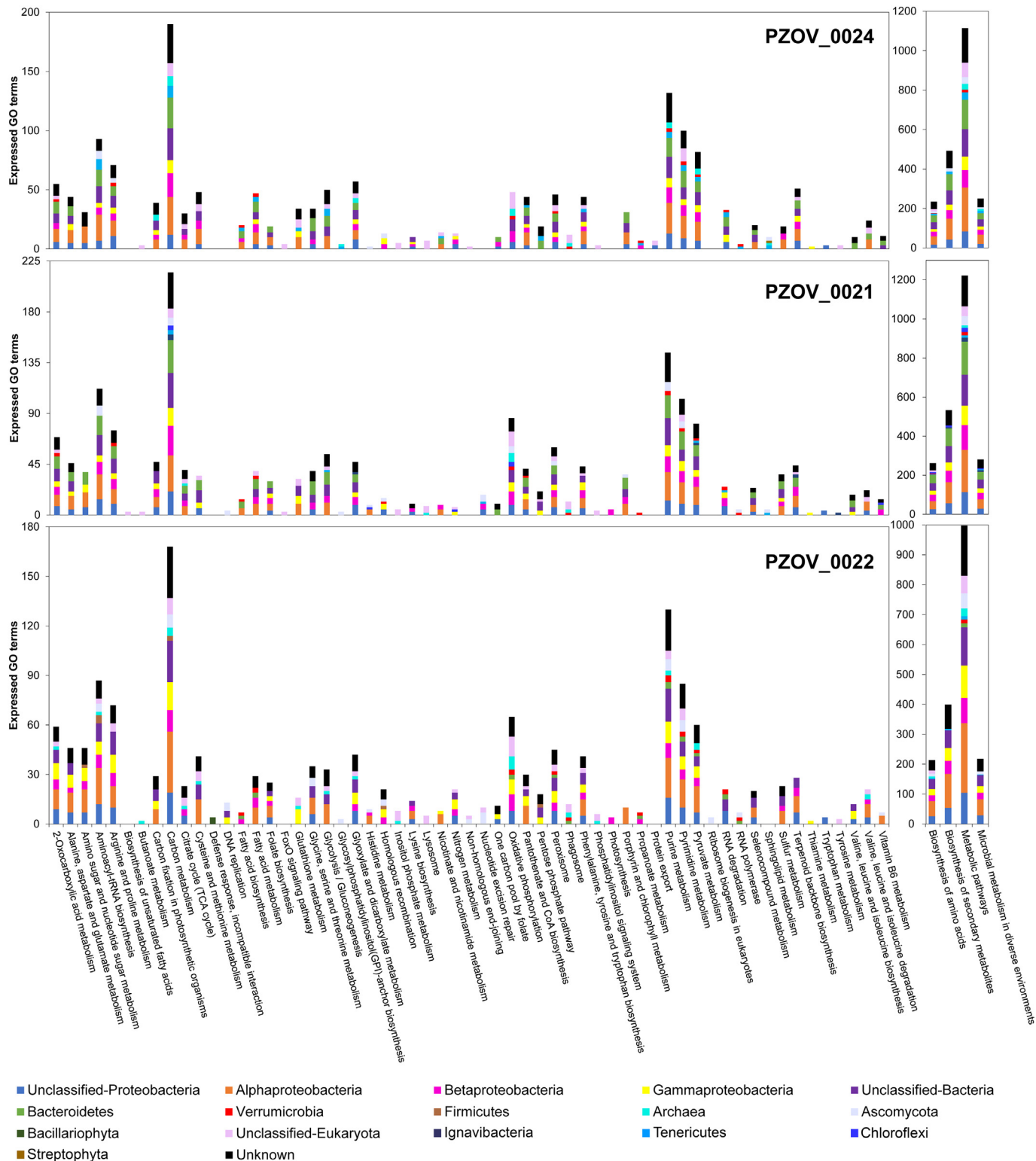


Fig. 7. Gene expression profile in the reduced water samples. Transcripts annotated with Gene Ontology (GO) “Biological Process” terms and enriched to KEGG database are shown. GO processes assigned to a phylum (or other taxonomical classification) of <1 % of the total were integrated as *Bacteria*, *Archaea*, or *Eukarya*.

were identified with 19, 36, and 23 GO-terms in these reduced water samples, and the transcripts were attributed to *Proteobacteria* (*Alpha*, and *Beta*), unclassified-*Bacteria*, and unknown-organisms in PZOV_0024 and PZOV_0022, and to *Proteobacteria* (*Alpha*, *Gamma*, and *Beta*), *Bacteroidetes*, unclassified-*Bacteria*, and unknown-organisms in PZOV_0021. Nitrogen metabolism was expressed by 13, 7 and 21 GO-terms attributed mainly to

Proteobacteria (*Beta*, *Gamma*, and unclassified), and unclassified-*Eukaryota* in PZOV_0024, to *Gammaproteobacteria*, *Chloroflexi*, and unclassified-*Eukaryota* in PZOV_0021, and to *Gammaproteobacteria* in PZOV_0022, and to *Proteobacteria* (*Beta*, *Gamma*, and unclassified), unclassified-*Bacteria* and -*Eukaryota* in PZOV_0022. Both purine and pyrimidine metabolisms from the “Nucleotide metabolism” were expressed in these reduced water

samples and particularly enriched in the PZOV_0021 water sample. mRNA transcripts were identified for Genetic Information Processing, including transcription with the pathway RNA polymerase attributed to *Tenericutes*, and *Verrumicrobia* in PZOV_0024, to *Verrumicrobia* and *Ascomycota* in PZOV_0021, and to *Bacteroidetes*, *Verrumicrobia* and *Ascomycota* in PZOV_0022, and Basal transcription factors only in PZOV_0021 expressed by *Ascomycota*; active translation was represented by the pathways for Aminoacyl-tRNA biosynthesis (93, 112, and 87 GO-terms) assigned in all three samples to all active Prokaryotes classified here with the exception of *Verrumicrobia*, beside *Archaea*, *Eukaryota* and unknown-organisms. Ribosome biogenesis in Eukaryotes was only found in PZOV_0022 and assigned to *Ascomycota*. Pathways for RNA degradation (33, 25, and 21 GO-terms) attributed to *Proteobacteria* (*Gamma*, and unclassified), *Tenericutes*, *Verrumicrobia*, *Bacteroidetes* and unclassified-*Bacteria* in PZOV_0024, to *Proteobacteria* (*Beta*, *Gamma*, and unclassified), *Tenericutes*, and *Verrumicrobia* in PZOV_0021, and to unclassified-*Proteobacteria*, *Verrumicrobia*, and *Bacteroidetes* in PZOV_0022. In addition, some transcripts encoding pathways for Protein export (in PZOV_0024 by unclassified-*Proteobacteria* and -*Eukaryota*), and Proteasome, which were also slightly expressed in PZOV_0021 by unclassified-*Eukaryota*. Replication and repair was mainly represented by pathways for Homologous recombination 13, 15, and 21 GO-terms attributed to *Proteobacteria* (*Beta*, and *Gamma*), and *Ascomycota* in PZOV_0024, to *Proteobacteria* (*Gamma*, and unclassified), *Verrumicrobia*, and *Ascomycota* in PZOV_0021, and to *Proteobacteria* (*Beta*, and *Gamma*), *Firmicutes*, *Ascomycota* and unknown-organisms in PZOV_0022, in addition to DNA replication (4 and 13 GO-terms in PZOV_0021 attributed to *Ascomycota* and in PZOV_0022 attributed to *Gammaproteobacteria*, unclassified-*Bacteria* and *Ascomycota*), and Nucleotide excision repair [18 and 10 GO-terms in PZOV_0021 attributed to *Proteobacteria* (*Beta*, and unclassified), *Tenericutes*, and *Ascomycota*, and in PZOV_0022 attributed to *Ascomycota*, and unclassified-*Eukaryota*].

Other metabolisms expressed by the active community members based on mRNA transcripts are detailed in the supplementary material S2.

3.4. Main genes expressed in the different redox compartments and classified in relation to the stress resulting from the redox U roll front zonation

Fig. 8 showed a more detailed examination of the functional groups' abundance, in which in addition to the presence of genes for N, S, P, and C metabolisms, the expression of several genes involved in the resistance to different stresses were observed as a result of the harsh environment of the U roll front for the microbial community. These resistance genes were probably forced by the presence in these waters of specific elements such as heavy metals and radionuclides (U, Ra, Se, As, Mn, Mo, etc.) in the mineralized and the oxidized compartments. Soluble metals would precipitate abiotically and biotically at the boundary between the oxidized and the mineralized zones, where they become insoluble due to the reducing conditions. Besides, several genes for environmental stress such as genes for the oxidative stress, DNA damage repair, and low pH adaptation were expressed with increasing levels from the oxidized to the reduced and the mineralized waters (Min > Red > Ox). Accumulation of such resistance genes seems to occur as a basic survival strategy used by the microbial communities in response to the harsh and oligotrophic conditions in the aquifers containing the U roll-front deposit.

4. Discussion

From the metatranscriptomic analysis of the aquifers surrounding U roll-front deposits, it is clear that microorganisms from all three domains of life (*Bacteria*, *Archaea*, and *Eukaryote*) are active and adapted to their environment (Fig. 9). Understanding the mechanisms by which they survive in such specific environments (low DOC, P, N, but high S and salinity) will enable us to shed light on their physiology and the strategies they hold to deal with U roll front deposit formation. In fact, such information would be crucial for the clarification of the important role that the microbial population could play in the genesis of U roll front type deposit under low temperatures. Concurrently, our results would help in understanding

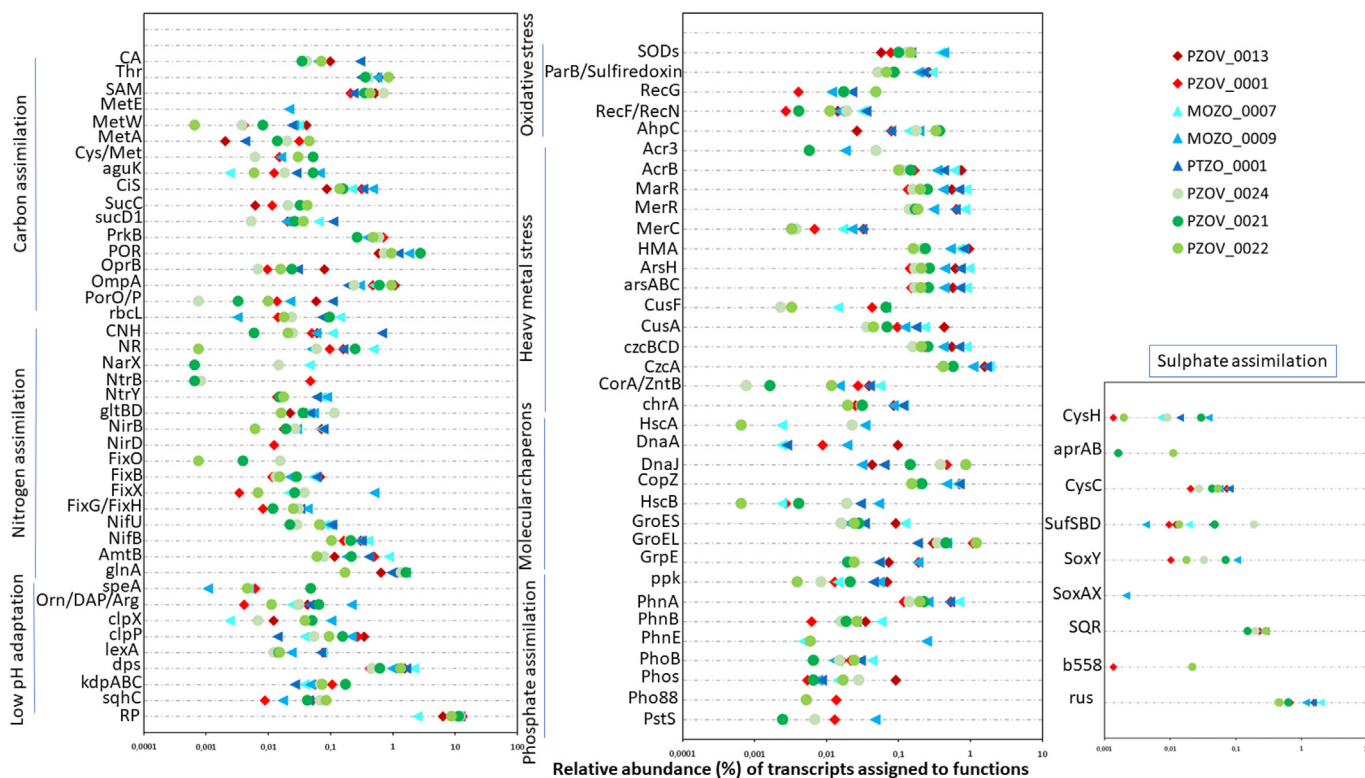


Fig. 8. Percentage of transcripts relative abundance associated with the *in situ* microbial functional metabolisms detected in the eight water samples. The bar showing the relative abundance was log scaled.

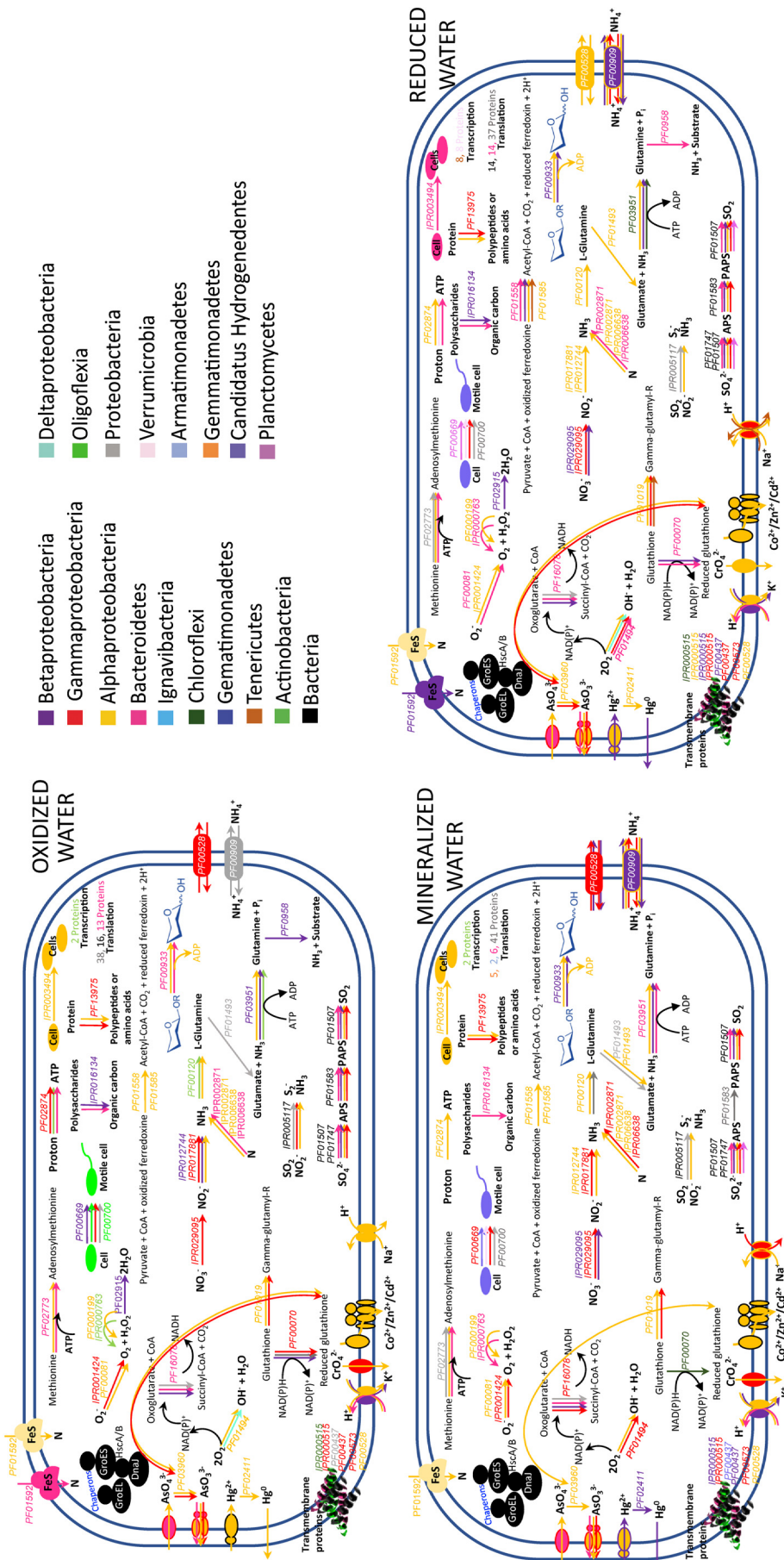


Fig. 9. Metabolic model showing the active pathways in the oxidized, the mineralized and the reduced waters. All processes were based on Gene Ontology (GO) terms and include some relevant InterProScan and Pfam classifications. Only major processes are shown for all water types. Processes associated to a phylum (or other taxonomical classification) are colour coded. Gene ID are also related by colours to the microbial phylum/Class.

their reactivity when the newly established extreme geochemical conditions related to ISR (i.e., acidification, solubilization of U and metals) are present. In such conditions, different stresses induced by metals, pH (oxidation), and the high sulfur are likely to impact the bacterial populations, mainly by enhancing the distribution of acidophilic microorganisms, sulfur/sulfate- and metal-metabolizers. Therefore, this work also focused on the analysis of key ecological and geochemical processes (N, S, C, and P) as well as other important functional genes such as metal resistance genes that transform the metal (oxidases, reductases, and transferases), oxidative stress genes, microbial defence genes, and low pH adaptation genes.

4.1. Relevant lifestyles involved by the resident bacteria in the U roll-front system

Bacteria are distributed and they are active in the different redox zonation (Figs. 8 and 9), where each activity is expressed by different microorganisms depending on this redox roll front zonation. In general, a shift in the functional gene composition was observed and was more pronounced in the mineralized and reduced compartments than in the oxidized (oxic) one. This can be explained by the fact that contamination increased from the oxidized to the reduced and the mineralized compartments (Jroundi et al., 2020).

4.1.1. Metal resistance

Shifts in the relative abundance of metal resistance genes were observed in this study, increasing from the reduced to oxidized and mineralized waters (Min > Ox > Red). This was in accordance with our previous observation that the concentration of heavy metals at the Zoovch Owoo site was higher in the mineralized compartment (rich in U, Mn, Fe, and Se), than in the oxidized one (Jroundi et al., 2020). These groundwaters are therefore unfit for human consumption with high levels of metalloids, exceeding the permissible levels for drinking waters (Ariunbileg et al., 2016). In a roll front system, dissolved heavy metals are occurring in equilibrium with the surrounding minerals and the specific U ore. Soluble metals would precipitate at the boundary between the oxidized and the reduced zone, where they become insoluble due to the reducing conditions. An explanation to this process could be that in the mineralized zone there is a massive Sulfur precipitation and presence of metallic Sulfur, in contrast to what occurs in the oxidized zone, where metals are soluble and transported to the mineralized compartment.

Many crucial genes conferring resistance to metals/radionuclides were observed in these water samples expressed by different bacteria (Figs. 8 and 9). Gene clusters for cobalt-zinc-cadmium (*czcBCD*, and *czcA*), As (*arsABC*, *acr3*, *arsH*), Cr (*chrA*), Hg (*merR*, *merC*) and Cu (*cusA*, *cusF*) resistance indicated elevated activity to survive in environments such as those of the U roll front deposit. Bacteria living in these waters are probably able to resist high heavy metal concentrations by genes encoding for *CzcA*, which is essential for the expression of cadmium, cobalt, and zinc resistance and play an important role in the export of redox-inactive metals (Co, Zn, and Cd) from several bacteria (Nies, 2003). Such system was also previously described in presence of 100 μM of uranyl acetate in *Ralstonia metallidurans* (Nies, 2003) and *Geobacter sulfurreducens* proteome (Orellana et al., 2014). Besides, Pinel-Cabello et al. (2021) described an up-regulation in the expression of *CzcA/CusA* and *CzcD* in *Stenotrophomonas bentonitica* treated with 100 μM of U, highlighting the importance of *CzcCBDA* complex in U tolerance. Additionally, resistance to mercury is detected by the presence of *MerR*, *MerT* and *MerC* (Dash et al., 2017; Sone et al., 2013), while resistance to arsenic in these waters could be conferred by its extrusion from the cells through the protein *Acr3* (Fu et al., 2009), in addition to the chromosomal resistance system *arsABC* and *arsH*. Reduction of arsenate to arsenite must occur before its transport out of the cell (Carlin et al., 1995). Therefore, the arsenate reductase *ArsC* uses a reduced glutathione (GSH) and glutaredoxin for the catalysis of such reaction (Liu and Rosen, 1997; Martin et al., 2001) (Fig. 9). The presence of these genes suggested a high activity of these bacterial communities in the As biotransformation and resistance at uranium roll-front environments. In those water samples, where the concentration of As is below detection limit (e.g.: MOZO_0007

and MOZO_0009), the expression of genes for As detoxification might be explained by the fact that this element shares structural similarities with selenium (Se) (Stolz et al., 2002). Consequently, both elements would share the same detoxification mechanisms. Selenium could be transported using the import system for As, then reduced by *ArsC*, and extruded from the cells by the arsenical efflux pump *ArsB*. Oxidative stress generated by the oxyanions would be prevented by the expression of the NADPH-dependent FMN oxidoreductase *ArsH* (Hervás et al., 2012; Pinel-Cabello et al., 2022).

Furthermore, expression of genes encoding for metal transport systems were found to be prevalent in all water samples, with a slight increase in the mineralized compartment. There is a Mg^{2+} transporter protein (*CorA*-like)/Zinc transport protein (*ZntB*) (*CorA/ZntB*) that accumulates divalent heavy metal ions non-specifically within the bacterial cells (Nanda et al., 2019), and a multidrug exporter *AcrB* responsible for the resistance of many microorganisms to wide range of drugs and antibiotics (Sennhauser et al., 2006; Wang et al., 2011). It was also detected here the expression of genes encoding for a cation efflux system *CzcA/CusA/SilA/NccA/HelA/CnrA* that consists of H^+ /heavy metal cation antiporters. This family mediates resistance to silver and copper with *CusA* and *SilA* (Franke et al., 2003; Outten et al., 2001), to several heavy metals like cadmium, nickel, and cobalt (*NccA*), catalyzes an energy-dependent efflux of Ni^{2+} and Co^{2+} (*CnrA*), and may be involved in the efflux of an unidentified substrate (with *HelA*). Furthermore, resistance to Ni and Co in these waters was also conferred by the Ni/Co homeostasis protein *RcnB* in conjunction with the efflux pump *RcnA* (Blériot et al., 2011).

In these water samples Ni, Cd, Zn, and Co concentrations are below detection limits and probably, bacteria use such genes expressed here (e.g.: transporters) as a mechanism for the maintenance of metal cation homeostasis to avoid U and other heavy metal toxicity by exporting them out from the cells (Pinel-Cabello et al., 2021). After ISR mining operation, high metal concentrations are expected to occur in solution as they are more soluble in acidic and oxidizing conditions. The identified genes suggest that bacteria would resist the high concentrations of metals generally observed after ISR.

4.1.2. Adaptation to stress

The expression of all the previous genes may suggest that after ISR activations, such active microbial community would be able to involve multiple adaptations to survive under elevated stress driven by the harsh acidic conditions, and neutralize the aquifer to pre-mining conditions after mining operations. Notably, from our results, it has been observed that bacteria express more responses to stress in the mineralized and the reduced waters than in the oxidized one. Systems to protect the cells from lysis and preserve the intracellular chemiosmotic gradient were encountered here. This is performed by using mechanisms such as protons' consumption by decarboxylation of amino-acid, metabolism of organic acids, and transport of protons between the cytoplasm and periplasm (Bearson et al., 1997; Hemme et al., 2010). For instance, in the case of acidic conditions, which should be prevailing after injection of sulfuric acid, the cells could adapt to the low pH by protons and other small ions' transport (for example K^+). Such adaptation could be conferred by *Orn/DAP/Arg* decarboxylase and Arginine decarboxylase (*speA*) implicated in the consumption of protons by decarboxylation of these amino-acids, and by the high affinity of K^+ translocating in *Kdp* complex (*KdpABC*); attributed here to *Fluviicola* and *Novosphingobium*. The expression of such genes is probably due to the high concentration of salinity in these water samples (Jroundi et al., 2020). Aside from protons and other ion transport, many proteins related to the DNA repair were expressed in these waters including Ribosomal proteins, Squalene/phytoene synthase (for substrate binding and/or catalytic mechanism), the transcriptional repressor *LexA*, in addition to *RecA*, both implicated in the SOS response to DNA damage. The presence of DNA-binding proteins *Dps*, synthesized during prolonged starvation to protect DNA from oxidative damage, was observed indicating the harsh conditions and oligotrophic environment at this site. The expression of genes related to several molecular chaperons, including *GroEL*, *GroES*, *GrpE*, *CopZ*, *DnaJ*,

DnaA, DnaK, and components of the ISC system (HscA and HscB) were abundantly expressed in the mineralized and reduced waters, indicating the need of these bacterial communities for a strong assistance from molecular chaperons to adequately cope with the environmental stress and repair of the damaged proteins (Okamoto-Kainuma and Ishikawa, 2016). Thus, the bacterial physiological feature on stress tolerance has been enhanced by the presence of genes involved in active chaperons and response to stress (Hong et al., 2012) as well as genes involved in DNA synthesis and replication (e.g.: DnaJ, and DnaA).

Noteworthy was the multiple processes employed by this active bacterial community as a response to the oxidative stress (also resulting from heavy metal pressure) and the maintenance of cell homeostasis (Chen et al., 2018; Nanda et al., 2019). Some oxidant and free radical detoxification processes strongly demand cells through the expression of genes encoding antioxidant compound synthesis (glutathione), peroxidase, superoxide dismutase (SOD), catalase, and peroxiredoxin (Figs. 8 and 9); mainly through the expression of Alkyl hydroperoxide reductase C (AhpC), Rec genes, and ParB/Sulfiredoxin proteins (Seaver and Imlay, 2001; Janion, 2008; Figge et al., 2003). Finally, the cell machineries were essentially powered by metabolic pathways such as tricarboxylic acids (TCA), glyoxylate, and pentose phosphate cycles, which consistently, with the other observed functions, are known to be involved in oxidants fighting and cell homeostasis (Amato et al., 2019; Oka et al., 2012).

4.1.3. Nitrate metabolism

Nitrate—present in these waters in moderately high concentrations (ranging from 1.02 to 14.87 mg/L)—is firstly consumed by nitrate-reducing bacteria as terminal electron acceptor to be gradually converted to N_2 . Bacteria in these waters metabolize more N in the mineralized and the oxidized waters than in the reduced ones. The concentration of N in form of NO_3 and NH_4 were distributed in function of the redox compartments, being more elevated in the oxidized waters (Jroundi et al., 2020 and Fig. S7). For this reason, it was expected to obtain a bacterial population especially active (high N assimilation genes) for the reduction of NO_3 to Nitrogen, but also those recycling NO_3 to NO_2 and NH_4 . This could be explained by the presence of more important levels of organic matters at the mineralized compartments observed in the waters at this site (Jroundi et al., 2020) and actually known for U ore deposits (Rallakis et al., 2019).

In the subsurface environment, nitrate reduction is mainly driven by the microbial control of local biogeochemical conditions, involving favorable environmental conditions (e.g.: absence of dissolved oxygen and micronutrients) and demanding electron donors (Henson et al., 2017; Rivett et al., 2008). In these water samples, mRNA transcripts encoding for NirB (the large subunit) and NirD (the small subunit) of the enzyme for the assimilatory nitrite reductase activity (Schneider and Schmidt, 2005) were highly expressed in the mineralized and the oxidized waters, respectively. Assimilatory nitrate/nitrite reductases change nitrate to nitrite to ammonium. The activity of nitrite reductase in *Actinobacteria* and *Proteobacteria* is carried out by this NADH-dependent nitrite reductase, neutralizing the nitrite produced during the nitrate reduction. NarX, a histidine kinase receptor, responds to the presence of nitrite and nitrate for the effective anaerobic respiration regulation in several bacteria (Cheung and Hendrickson, 2009). Also, prevalent here were transcripts for Nitrite/Sulfite reductase 4Fe-4S domain, which catalyze the six-electron reductions of sulfite to sulfide, and nitrite to ammonia, respectively. Ammonium transport is then assumed by the AmtB protein (Khademi et al., 2004) expressed abundantly in these water samples. Also detected here were nitrogen regulation (NR) proteins phosphorylated by NtrB, a two-component regulatory system for the transcription of glnA (Rexer et al., 2006), a key enzyme implicated in nitrogen metabolism, that acts in both nitrogen assimilation and L-glutamine biosynthesis, involving gltBD (Chen et al., 2015).

Nitrogen fixation is also usually employed as a strategy for the bacterial survival in metal-rich oligotrophic mining environments (Sun et al., 2020). In fact, in all these water samples, many genes for nitrogen fixation are expressed encoding for NifU, and NifB, from the NIF system needed for

the production of metalloclusters of nitrogenase, the nitrogen-fixing enzyme, that catalyzes the nitrogen fixation in several microorganisms (Allen et al., 1995; Seidler et al., 2001). Also, genes encoding for FixO, FixX, FixH, and FixG were highly expressed (Figs 8 and 9). Among them was the FixO as a subunit of cytochrome cbb3 oxidase that provides oxygen reduction in suboxic environments with its high-oxygen-affinity. FixX, a Ferredoxin-like protein (one of the nitrogen-fixation genes locus of various species), suggested to donate electrons to nitrogenase. Instead, FixH and FixG are thought to be involved in a membrane-bound complex, coupling a redox process with the cation pump (FixI) catalyzed by FixG (Kahn et al., 1989).

Nitrate assimilation, in this extreme environment, could have an important role in the reduction of U(VI) to U(IV) and therefore, positively affect uranium bioremediation, since no radionuclide reduction was reported to occur in nitrate- and uranium-containing environments prior to complete nitrate removal (Safonov et al., 2018). Moreover, SO_4 reduction is limited as long as NO_3 is still present in the environment (Davidova et al., 2001; He et al., 2010). Specific stress could be posed to sulfate reducing bacteria (SRB) by the presence of nitrate as this element has been observed to suppress the *in situ* sulfate reduction (Jenneman et al., 1986). Thus, the presence of such active nitrate assimilating bacteria would actually promote the activity of SRB.

4.1.4. Sulfur/sulfate metabolism

The mineralogical composition of Zoovch Ovoo deposits sandy sediments showed the presence of some biogenic framboidal pyrite (FeS_2) in the fine sedimentary matrix (Robin et al., 2020; Rallakis et al., 2019). The dissolution of such Sulfur-bearing minerals may result in a Sulfur-rich environment, where variations in the different Sulfur elements would contribute to the biogeochemical Sulfur cycling. Large number of functional genes responsible for Sulfur cycling were detected in the different aquifer compartments at this site (Figs 8 and 9), being more pronounced in the reduced and mineralized compartments than in the oxidized one. Sulfate-reducing bacteria were particularly active since important genes were retained for sulfate reduction namely the sulfate dissimilating reductase aprAB (Adenylylsulfate reductase, assigned to unclassified-*Bacteroidetes*), two sulfate assimilation reductases: APS [adenylylsulfate kinase (cysC)] and PAPS reductase [Phosphoadenosine phosphosulfate reductase (cysH)], and a SAT [Sulfate adenylyltransferase (cysN)]. In this study, the abundance of sulfate assimilating reductases was much higher than that of sulfate dissimilating reductases (absence of *dsr* genes), indicating that the microbial community involved a strong Sulfur assimilation effect for the sulfate reduction. Several sulfate-assimilating bacteria use APS as the substrate for sulfate reduction (Ayangbenro et al., 2018; Bick et al., 2000). Meanwhile, the abundance of one of the key enzymes for dissimilatory sulfur reduction, sulfate dissimilating reductases (aprAB), which transform sulfate to sulfide under anoxic conditions, indicated the implication of this community in the reduction of sulfate, using it as a terminal electron acceptor for respiration in the absence of molecular oxygen (Biderre-Petit et al., 2011). Sulfate reduction can increase pH by consuming protons coupled with the precipitation of toxic metals as metal sulfides (Ayangbenro et al., 2018). Thus, sulfate-reducing bacteria play a crucial role in generating alkalinity and neutralizing acidic environments such as those impacted by the ISR process. According to Sun et al. (2020), an elevated abundance of functional genes for sulfate reduction was detected in the more highly contaminated Acid Mine Drainage (AMD) site with a pH value of 2.5, indicating the presence and activity of such SRB in these extreme pH environments. This could be explained by the detected activity of acidophilic bacteria, which are able to oxidize reduced sulfur compounds (e.g.: thiosulfate, Sulfur, etc.) occurring in metal sulfides such as pyrite, FeS_2 , and providing sulfates that enhance the growth of SRB. In addition, such SRB could have a significant implication in the genesis of the U deposits in the mineralized compartment, by providing sulfides as a reducing agent or generating biogenic U necessary for the construction of the roll front ore deposit (Bhattacharyya et al., 2017).

4.2. Implications of the active microbial communities in the U roll-front environments

Our metatranscriptomic analysis has provided a detailed gene transcriptional profile for the naturally occurring microbial communities in this extreme U roll-front deposit environment, demonstrating how these microorganisms could change and adapt to the different physiological conditions (Fig. 9). The transcriptional analysis revealed a high diversity of transcripts closely related to the physicochemical characteristics of the roll-front deposit environment, being slightly more pronounced at the mineralized and reduced aquifer compartments. Furthermore, significant functions, biogeochemical pathways and important processes involved in the genesis of the sandstone-hosted roll-front U deposits at low-temperature like those of the Zoovch Ovoo deposit could be elucidated here. Presence and activity of some key microorganisms such as active sulfate-reducing bacteria at the mineralized compartments supports the implication of the biogenic processes in the U ore genesis in the roll-front deposits. In fact, Rallakis et al. (2021) recently proposed a comprehensive metallogenic model for the uranium ore genesis at the Zoovch Ovoo deposit, and suggested that U trapping and reduction occur mainly through biomineralization processes by the continuous bacterial activity and sulfides liberated as a by-product from the pyrite bio-oxidation. In this study, for the first time, the transcriptional bacterial activity was demonstrated in the redox controlled aquifer system, which supports the evidences that a significant role is played by the found active bacteria in the direct U trapping and concentration as reducing agents. These findings would help to dissipate the doubts about the microbial role in the U ore genesis and the further implications of the biogenic processes in U ore or pyrite formation.

Moreover, from the detection of transcripts for heavy metal-, nitrate-, and sulfate-reduction as well as genes for the adaptation to acid pH, important clues are provided for such activities within the aquifer. Overall, the transcriptional behaviour of the microbial communities (sulfur oxidation, sulfate reduction, nitrate reduction, heavy metal reduction, etc.) indicates their versatility and adaptability in the aquifer, while redox and geochemical conditions change. It also gives important insights into their contribution to the stabilization of these U roll-front environments and the potential further implication in the aquifer restoration to the initial pre-mining conditions after an ISR actuation. Furthermore, in the hypothetical case of increasing concentrations of heavy metals such as Cd, As, Hg or other trace metals, that result from the dissolution of U orebody minerals during the ISR process, the microbial communities showed the ability of adopting many resistance approaches that impact directly the transport and transformation of such metals/radionuclides (e.g.: U) by affecting their speciation and solubility and thus decreasing their toxicity in the environment (Macur et al., 2001; Sun et al., 2018; Yan et al., 2020; Yang et al., 2016).

All in all, the data presented in this study further demonstrate that the future uranium remediation would probably be achieved by the occurring of metal-reducing bacteria, enhanced and facilitated by nitrate and sulfate reduction activities. Geochemical conditions in the natural roll front environment (Eh, metal gradient, pH, O₂, etc.) would govern the bacterial identity as well as their abundance, which in turn influence the activities expressed in each zone. In general, the oxidized oxic conditions seem to induce less stress responses in the bacterial populations than in the anoxic mineralized and reduced conditions. Thus, it is worth to indicate, that the stress responses observed would be related to the structure of the roll front. Such observation highlights that determining the bacterial activity and not only diversity, is the most suitable way for providing accurate information on roll front zonation and orebody formation. More importantly, insights into the transcriptional traits of the microbial communities and their adaptation in response to the changing environmental conditions are definitely imperative challenges to elucidate for the correct application of bioremediation strategies.

5. Conclusions

In summary, our metatranscriptomic study from groundwaters of a U roll-front deposits illuminated structural and functional variations among the different redox-inferred aquifer compartments. We provide here the first molecular picture including important information on the functioning of microbial living cells, their physiological adaptabilities and potential impacts within such environments before any mining ISR actuations. This help to highlight interesting biological functions, and allows to accurately identify specific target genes for futures investigations. Overall, this study helps to define the actual biological imprints on U roll-front environments and predict clues about the microbial activity that will be induced by post-operational environmental factors. Additionally, it provides key information for the understanding of the role of the active microorganisms in the genesis of U deposits under low temperatures. In particular, high expression of transcripts associated with wide range of functions was detected. Interestingly, *Bacteria*, *Archaea*, and *Eukarya* are demonstrated to play a crucial role in several processes like nitrogen metabolism, sulfur metabolism, heavy-metal resistance, carbon metabolism, oxidative and environmental stress in the U roll-front deposits, regardless of the type of redox inferred in each aquifer compartment. Finally, this study indicated the adaptability of the microbial communities to the changing geochemical conditions in such an extreme environment as shown by the presence of key genes associated to the resistance to specific elements and stresses. Through the performance of this type of analyses, we could clarify the microbial metabolic lifestyles and expression patterns in a U roll-front system, thereby expanding our assessment of the microbial capabilities and limitations, in view of a suitable remediation scenario.

Supplementary data to this article can be found online at <https://doi.org/10.1016/j.scitotenv.2022.160636>.

CRedit authorship contribution statement

Fadwa Jroundi: Conceptualization, Methodology, Investigation, Verification, Formal analysis, Data Curation, Writing - original draft; Writing - Review & Editing. **Cristina Povedano-Priego:** Methodology, Investigation, Validation, Formal analysis, Visualization. **María Pinel-Cabello:** Methodology, Investigation. **Michael Descostes:** Conceptualization, Supervision, Methodology, Resources, Funding acquisition, Writing - original draft, Writing - Review and Editing. **Pierre Grizard:** Resources. **Bayaarma Purevsan:** Resources. **Mohamed L. Merroun:** Conceptualization, Supervision, Methodology, Resources, Project administration, Funding acquisition, Writing - original draft, Writing - Review and Editing.

Data availability

I have shared the access number of my data in the main text of the manuscript.

Declaration of competing interest

The authors declare that they have no known competing financial interests or personal relationships that could have appeared to influence the work reported in this paper.

Acknowledgements

We thank the local hydrogeological team from Badrakh Energy for providing access to piezometers and for their contribution to the sampling process. We also knowledge the "Universidad de Granada / CBUA" for the funding of the open access charge."

Funding

Financial support for this research was provided by ORANO Mining (France) through the collaborative research contract n° 3748 (OTRI).

References

- Akhtar, S., Yang, X., Pirajno, F., 2017. Sandstone type uranium deposits in the Ordos Basin, Northwest China: a case study and an overview. *J. Asian Earth Sci.* 146, 367–382. <https://doi.org/10.1016/j.jseaes.2017.05.028>.
- Allen, R.M., Chatterjee, R., Ludden, P.W., Shah, V.K., 1995. Incorporation of iron and sulfur from NiB cofactor into the iron-molybdenum cofactor of dinitrogenase. *J. Biol. Chem.* 270, 26890–26896. <https://doi.org/10.1074/jbc.270.45.26890>.
- Amato, P., Besaury, L., Joly, M., Penaud, B., Deguillaume, L., Delort, A.-M., 2019. Metatranscriptomic exploration of microbial functioning in clouds. *Sci. Rep.* 9, 4383. <https://doi.org/10.1038/s41598-019-41032-4>.
- Ariunbileg, S., Gaskova, O., Vladimirov, A., Battushig, A., Moroz, E., 2016. Spatial distribution of uranium and metalloids in groundwater near sandstone-type uranium deposits, southern Mongolia. *Geochem. J.* 50, 393–401. <https://doi.org/10.2343/geochemj.2.0434>.
- Ayangbenro, A.S., Olanrewaju, O.S., Babalola, O.O., 2018. Sulfate-reducing bacteria as an effective tool for sustainable acid mine bioremediation. *Front. Microbiol.* 9. <https://doi.org/10.3389/fmicb.2018.01986>.
- Bearson, S., Bearson, B., Foster, J.W., 1997. Acid stress responses in enterobacteria. *FEMS Microbiol. Lett.* 147, 173–180. <https://doi.org/10.1111/j.1574-6968.1997.tb10238.x>.
- Bhattacharyya, A., Campbell, K.M., Kelly, S.D., Roebbert, Y., Weyer, S., Bernier-Latmani, R., Borch, T., 2017. Biogenic non-crystalline U (IV) revealed as major component in uranium ore deposits. *Nat. Commun.* 8, 15538. <https://doi.org/10.1038/ncomms15538>.
- Bick, J.A., Dennis, J.J., Zylstra, G.J., Nowack, J., Leustek, T., 2000. Identification of a new class of 5'-adenylsulfate (APS) reductases from sulfate-assimilating bacteria. *J. Bacteriol.* 182, 135–142. <https://doi.org/10.1128/JB.182.1.135-142.2000>.
- Bidder-Petit, C., Boucher, D., Kuever, J., Alberic, P., Jézéquel, D., Chebance, B., Borrel, G., Fonty, G., Peyret, P., 2011. Identification of sulfur-cycle prokaryotes in a low-sulfate Lake (Lake Pavin) using *aprA* and 16S rRNA gene markers. *Microb. Ecol.* 61, 313–327. <https://doi.org/10.1007/s00248-010-9769-4>.
- Blériot, C., Effantin, G., Lagarde, F., Mandrand-Berthelot, M.-A., Rodrigue, A., 2011. RcnB is a periplasmic protein essential for maintaining intracellular Ni and Co concentrations in *Escherichia coli*. *J. Bacteriol.* 193, 3785–3793. <https://doi.org/10.1128/JB.05032-11>.
- Bolger, A.M., Lohse, M., Usadel, B., 2014. Trimmomatic: a flexible trimmer for illumina sequence data. *Bioinform. Oxf. Engl.* 30, 2114–2120. <https://doi.org/10.1093/bioinformatics/btu170>.
- Bonnetti, C., Liu, X., Zhaobin, Y., Cuney, M., Michels, R., Malartre, F., Mercadier, J., Cai, J., 2017. Coupled uranium mineralisation and bacterial sulphate reduction for the genesis of the baxingtou sandstone-hosted U deposit, SW Songliao Basin NE China. *Ore Geol. Rev.* 82, 108–129. <https://doi.org/10.1016/j.oregeorev.2016.11.013>.
- Burns, P.C., Finch, R.J., 2018. Uranium: Mineralogy, Geochemistry, and the Environment. Walter de Gruyter GmbH & Co KG.
- Cambuy, D.D., Coutinho, F.H., Dutilh, B.E., 2016. ContigAnnotation Tool CAT Robustly Classifies Assembled Metagenomic Contigs and LongSequences. *bioRxiv* <https://doi.org/10.1101/072868>.
- Carlin, A., Shi, W., Dey, S., Rosen, B.P., 1995. The *ars* operon of *Escherichia coli* confers arsenical and antimicrobial resistance. *J. Bacteriol.* 177, 981–986.
- Chen, L., Hu, M., Huang, L., Hua, Z., Kuang, J., Li, S., Shu, W., 2015. Comparative metagenomic and metatranscriptomic analyses of microbial communities in acid mine drainage. *ISME J.* 9, 1579–1592. <https://doi.org/10.1038/ismej.2014.245>.
- Chen, W., Teng, Y., Li, Z., Liu, W., Ren, W., Luo, Y., Christie, P., 2018. Mechanisms by which organic fertilizer and effective microbes mitigate peanut continuous cropping yield constraints in a red soil of south China. *Appl. Soil Ecol.* 128, 23–34. <https://doi.org/10.1016/j.apsoil.2018.03.018>.
- Cheung, J., Hendrickson, W.A., 2009. Structural analysis of ligand stimulation of the histidine kinase NarX. *Structure* 17, 190–201. <https://doi.org/10.1016/j.str.2008.12.013>.
- Coral, T., Descostes, M., De Boissezon, H., Bernier-Latmani, R., de Alencastro, L.F., Rossi, P., 2018. Microbial communities associated with uranium in-situ recovery mining process are related to acid mine drainage assemblages. *Sci. Total Environ.* 628–629, 26–35. <https://doi.org/10.1016/j.scitotenv.2018.01.321>.
- Coral, T., Placko, A.-L., Beaufort, D., Tertre, E., Bernier-Latmani, R., Descostes, M., De Boissezon, H., Guillon, S., Rossi, P., 2022. Biostimulation as a sustainable solution for acid neutralization and uranium immobilization post acidic in-situ recovery. *Sci. Total Environ.* 822, 153597. <https://doi.org/10.1016/j.scitotenv.2022.153597>.
- Cumberland, S.A., Douglas, G., Grice, K., Moreau, J.W., 2016. Uranium mobility in organic matter-rich sediments: a review of geological and geochemical processes. *Earth-Sci. Rev.* 159, 160–185. <https://doi.org/10.1016/j.earscirev.2016.05.010>.
- Dash, H.R., Sahu, M., Mallick, B., Das, S., 2017. Functional efficiency of MerA protein among diverse mercury resistant bacteria for efficient use in bioremediation of inorganic mercury. *Biochimie* 142, 207–215. <https://doi.org/10.1016/j.biochi.2017.09.016>.
- Davidova, I., Hicks, M.S., Fedorak, P.M., Sufitla, J.M., 2001. The influence of nitrate on microbial processes in oil industry production waters. *J. Ind. Microbiol. Biotechnol.* 27, 80–86. <https://doi.org/10.1038/sj.jim.7000166>.
- Descostes, M., Schlegel, M.L., Eglizaud, N., Descamps, F., Miserque, F., Simoni, E., 2010. Uptake of uranium and trace elements in pyrite (FeS₂) suspensions. *Geochim. Cosmochim. Acta* 74, 1551–1562. <https://doi.org/10.1016/j.gca.2009.12.004>.
- Figge, R.M., Easter, J., Gober, J.W., 2003. Productive interaction between the chromosome partitioning proteins, ParA and ParB, is required for the progression of the cell cycle in *Caulobacter crescentus*. *Mol. Microbiol.* 47, 1225–1237. <https://doi.org/10.1046/j.1365-2958.2003.03367.x>.
- Franke, S., Grass, G., Rensing, C., Nies, D.H., 2003. Molecular analysis of the copper-transporting efflux system CusCFBA of *Escherichia coli*. *J. Bacteriol.* 185, 3804–3812. <https://doi.org/10.1128/JB.185.13.3804-3812.2003>.
- Fu, H.-L., Meng, Y., Ordóñez, E., Villadangos, A.F., Bhattacharjee, H., Gil, J.A., Mateos, L.M., Rosen, B.P., 2009. Properties of arsenite efflux permeases (Acr3) from *Alkaliphilus metalliredigens* and *Corynebacterium glutamicum*. *J. Biol. Chem.* 284, 19887–19895. <https://doi.org/10.1074/jbc.M109.011882>.
- Ge, S.X., Jung, D., Yao, R., 2020. ShinyGO: a graphical gene-set enrichment tool for animals and plants. *Bioinformatics* 36, 2628–2629. <https://doi.org/10.1093/bioinformatics/btz931>.
- Grabherr, M.G., Haas, B.J., Yassour, M., Levin, J.Z., Thompson, D.A., Amit, I., Adiconis, X., Fan, L., Raychowdhury, R., Zeng, Q., Chen, Z., Mauceli, E., Hacohen, N., Gnirke, A., Rhind, N., di Palma, F., Birren, B.W., Nusbaum, C., Lindblad-Toh, K., Friedman, N., Regev, A., 2011. Trinity: reconstructing a full-length transcriptome without a genome from RNA-seq data. *Nat. Biotechnol.* 29, 644–652. <https://doi.org/10.1038/nbt.1883>.
- Granger, H.C., Warren, C.G., 1969. Unstable sulfur compounds and the origin of roll-type uranium deposits. *Econ. Geol.* 64, 160–171. <https://doi.org/10.2113/gsecongeo.64.2.160>.
- Grozeva, N.G., Radwan, J., Beaucaire, C., Descostes, M., 2022. Reactive transport modeling of U and Ra mobility in roll-front uranium deposits: parameters influencing 226Ra/238U disequilibria. *J. Geochem. Explor.* 236, 106961. <https://doi.org/10.1016/j.gexplo.2022.106961>.
- Gura, C., Rogers, S.O., 2020. Metatranscriptomic and metagenomic analysis of biological diversity in subglacial Lake Vostok (Antarctica). *Biology* 9, 55. <https://doi.org/10.3390/biology9030055>.
- He, Q., He, Z., Joyner, D.C., Joachimiak, M., Price, M.N., Yang, Z.K., Yen, H.-C.B., Hemme, C.L., Chen, W., Fields, M.M., Stahl, D.A., Keasling, J.D., Keller, M., Arkin, A.P., Hazen, T.C., Wall, J.D., Zhou, J., 2010. Impact of elevated nitrate on sulfate-reducing bacteria: a comparative study of *Desulfovibrio vulgaris*. *ISME J.* 4, 1386–1397. <https://doi.org/10.1038/ismej.2010.59>.
- He, Z., Zhang, P., Wu, Linwei, Rocha, A.M., Tu, Q., Shi, Z., Wu, B., Qin, Y., Wang, J., Yan, Q., Curtis, D., Ning, D., Nostrand, J.D.V., Wu, Liyou, Yang, Y., Elias, D.A., Watson, D.B., Adams, M.W.V., Fields, M.W., Alm, E.J., Hazen, T.C., Adams, P.D., Arkin, A.P., Zhou, J., 2018. Microbial functional gene diversity predicts groundwater contamination and ecosystem functioning. *mBio*, 9. <https://doi.org/10.1128/mBio.02435-17>.
- Hemme, C.L., Deng, Y., Gentry, T.J., Fields, M.W., Wu, L., Barua, S., Barry, K., Tringe, S.G., Watson, D.B., He, Z., Hazen, T.C., Tiedje, J.M., Rubin, E.M., Zhou, J., 2010. Metagenomic insights into evolution of a heavy metal-contaminated groundwater microbial community. *ISME J.* 4, 660–672. <https://doi.org/10.1038/ismej.2009.154>.
- Henson, W.R., Huang, L., Graham, W.D., Ogram, A., 2017. Nitrate reduction mechanisms and rates in an unconfined eogenetic karst aquifer in two sites with different redox potential. *J. Geophys. Res. Biogeosci.* 122, 1062–1077. <https://doi.org/10.1002/2016JG003463>.
- Hervás, M., López-Maury, L., León, P., Sánchez-Riego, A.M., Florencio, F.J., Navarro, J.A., 2012. ArsH from the cyanobacterium *Synechocystis* sp. PCC 6803 is an efficient nadp-dependent quinone reductase. *Biochemistry* 51, 1178–1187. <https://doi.org/10.1021/bi201904p>.
- Hong, W., Wu, Y.E., Fu, X., Chang, Z., 2012. Chaperone-dependent mechanisms for acid resistance in enteric bacteria. *Trends Microbiol.* 20, 328–335. <https://doi.org/10.1016/j.tim.2012.03.001>.
- Hu, Z., Bao, J., Reecy, J., 2008. CateGOrizer: a web-based program to batch analyze gene ontology classification categories. *Online J. Bioinform.* 9, 108–112.
- Hügler, M., Huber, H., Molyneux, S.J., Vetrani, C., Sievert, S.M., 2007. Autotrophic CO₂ fixation via the reductive tricarboxylic acid cycle in different lineages within the phylum Aquificae: evidence for two ways of citrate cleavage. *Environ. Microbiol.* 9 (1), 81–92.
- Hügler, M., Wirsén, C.O., Fuchs, G., Taylor, C.D., Sievert, S.M., 2005. Evidence for autotrophic CO₂ fixation via the reductive tricarboxylic acid cycle by members of the ϵ subdivision of Proteobacteria. *J. Bacteriol.* 187 (9), 3020–3027.
- IAEA, NEA, 2018. Uranium 2018: Resources, Production and Demand NEA7413 462.
- Janion, C., 2008. Inducible SOS response system of DNA repair and mutagenesis in *Escherichia coli*. *Int. J. Biol. Sci.* 4, 338–344.
- Jenneman, G.E., McInerney, M.J., Knapp, R.M., 1986. Effect of nitrate on biogenic sulfide production. *Appl. Environ. Microbiol.* 51, 1205–1211. <https://doi.org/10.1128/aem.51.6.1205-1211.1986>.
- Jewell, T.N.M., Karaoz, U., Brodie, E.L., Williams, K.H., Beller, H.R., 2016. Metatranscriptomic evidence of pervasive and diverse chemolithoautotrophy relevant to C, S, N and Fe cycling in a shallow alluvial aquifer. *ISME J.* 10, 2106–2117. <https://doi.org/10.1038/ismej.2016.25>.
- Jiang, W., Liang, P., Wang, B., Fang, J., Lang, J., Tian, G., Jiang, J., Zhu, T.F., 2015. Optimized DNA extraction and metagenomic sequencing of airborne microbial communities. *Nat. Protoc.* 10, 768–779. <https://doi.org/10.1038/nprot.2015.046>.
- Jin, R., Teng, X., Li, X., Si, Q., Wang, W., 2020. Genesis of sandstone-type uranium deposits along the northern margin of the Ordos Basin, China. *Geosci. Front.* 11, 215–227. <https://doi.org/10.1016/j.gsf.2019.07.005>.
- Jroundi, F., Descostes, M., Povedano-Priego, C., Sánchez-Castro, I., Suvannagan, V., Grizard, P., Merroun, M.L., 2020. Profiling native aquifer bacteria in a uranium roll-front deposit and their role in biogeochemical cycle dynamics: insights regarding in situ recovery mining. *Sci. Total Environ.* 721, 137758. <https://doi.org/10.1016/j.scitotenv.2020.137758>.
- Kahn, D., David, M., Domergue, O., Davaeran, M.L., Ghai, J., Hirsch, P.R., Batut, J., 1989. *Rhizobium melliotti* fixGHI sequence predicts involvement of a specific cation pump in symbiotic nitrogen fixation. *J. Bacteriol.* 171, 929–939.
- Khademi, S., O'Connell, J., Remis, J., Robles-Colmenares, Y., Miercke, L.J.W., Stroud, R.M., 2004. Mechanism of ammonia transport by Amt/MEP/Rh: structure of AmtB at 1.35 Å. *Science* 305, 1587–1594. <https://doi.org/10.1126/science.1101952>.
- Li, B., Dewey, C.N., 2011. RSEM: accurate transcript quantification from RNA-seq data with or without a reference genome. *BMC Bioinformatics* 12, 323. <https://doi.org/10.1186/1471-2105-12-323>.
- Li, D., Kaplan, D.L., Chang, H.-S., Seaman, J.C., Jaffé, P.R., Koster van Groos, P., Scheckel, K.G., Segre, C.U., Chen, N., Jiang, D.-T., Newville, M., Lanzirotti, A., 2015. Spectroscopic evidence of uranium immobilization in acidic wetlands by natural organic matter and plant roots. *Environ. Sci. Technol.* 49, 2823–2832. <https://doi.org/10.1021/es505369g>.
- Liu, J., Rosen, B.P., 1997. Ligand interactions of the ArsC arsenate reductase. *J. Biol. Chem.* 272, 21084–21089. <https://doi.org/10.1074/jbc.272.34.21084>.

- Lu, J., Salzberg, S.L., 2020. Ultrafast and accurate 16S rRNA microbial community analysis using kraken 2. *Microbiome* 8, 124. <https://doi.org/10.1186/s40168-020-00900-2>.
- Macur, R.E., Wheeler, J.T., McDermott, T.R., Inskeep, W.P., 2001. Microbial populations associated with the reduction and enhanced mobilization of arsenic in mine tailings. *Environ. Sci. Technol.* 35, 3676–3682. <https://doi.org/10.1021/es0105461>.
- Martin, P., DeMel, S., Shi, J., Gladysheva, T., Gatti, D.L., Rosen, B.P., Edwards, B.F.P., 2001. Insights into the structure, solvation, and mechanism of ArsC arsenate reductase, a novel arsenic detoxification enzyme. *Structure* 9, 1071–1081. [https://doi.org/10.1016/S0969-2126\(01\)00672-4](https://doi.org/10.1016/S0969-2126(01)00672-4).
- Min, M., Xu, H., Chen, J., Fayek, M., 2005. Evidence of uranium biomineralization in sandstone-hosted roll-front uranium deposits, northwestern China. *Ore Geol. Rev.* 26, 198–206. <https://doi.org/10.1016/j.oregeorev.2004.10.003>.
- Mtimunye, P.J., Chirwa, E.M.N., 2019. Uranium (VI) reduction in a fixed-film reactor by a bacterial consortium isolated from uranium mining tailing heaps. *Biochem. Eng. J.* 145, 62–73. <https://doi.org/10.1016/j.bej.2019.02.002>.
- Nanda, M., Kumar, V., Sharma, D.K., 2019. Multimetal tolerance mechanisms in bacteria: the resistance strategies acquired by bacteria that can be exploited to 'clean-up' heavy metal contaminants from water. *Aquat. Toxicol.* 212, 1–10. <https://doi.org/10.1016/j.aquatox.2019.04.011>.
- Nies, D.H., 2003. Efflux-mediated heavy metal resistance in prokaryotes. *FEMS Microbiol. Rev.* 27, 313–339. [https://doi.org/10.1016/S0168-6445\(03\)00048-2](https://doi.org/10.1016/S0168-6445(03)00048-2).
- Oka, S.-I., Hsu, C.-P., Sadoshima, J., 2012. Regulation of cell survival and death by pyridine nucleotides. *Circ. Res.* 111, 611–627. <https://doi.org/10.1161/CIRCRESAHA.111.247932>.
- Okamoto-Kainuma, A., Ishikawa, M., 2016. Physiology of *Acetobacter* spp.: involvement of molecular chaperones during acetic acid fermentation. In: Matsushita, K., Toyama, H., Tonouchi, N., Okamoto-Kainuma, A. (Eds.), *Acetic Acid Bacteria: Ecology and Physiology*. Springer Japan, Tokyo, pp. 179–199. https://doi.org/10.1007/978-4-431-55933-7_8.
- Orellana, R., Hixson, K.K., Murphy, S., Mester, T., Sharma, M.L., Lipton, M.S., Lovley, D.R., 2014. Proteome of *Geobacter sulfurreducens* in the presence of U(VI). *Microbiology* 160, 2607–2617. <https://doi.org/10.1099/mic.0.081398-0>.
- Outten, F.W., Huffman, D.L., Hale, J.A., O'Halloran, T.V., 2001. The independent cue and cus systems confer copper tolerance during aerobic and anaerobic growth in *Escherichia coli*. *J. Biol. Chem.* 276, 30670–30677. <https://doi.org/10.1074/jbc.M104122200>.
- Overholt, W.A., Trumbore, S., Xu, X., Bornemann, T.L.V., Probst, A.J., Krüger, M., Herrmann, M., Thandrup, B., Bristow, L.A., Taubert, M., Schwab, V.F., Hölzer, M., Marz, M., Küsel, K., 2022. Carbon fixation rates in groundwater similar to those in oligotrophic marine systems. *Nat. Geosci.* 15, 561–567.
- Pinel-Cabello, M., Jroundi, F., López-Fernández, M., Geffers, R., Jarek, M., Jauregui, R., Link, A., Vilchez-Vargas, R., Merroun, M.L., 2021. Multisystem combined uranium resistance mechanisms and bioremediation potential of *Stenotrophomonas bentonitica* BII-R7: transcriptomics and microscopic study. *J. Hazard. Mater.* 403, 123858. <https://doi.org/10.1016/j.jhazmat.2020.123858>.
- Pinel-Cabello, M., Jauregui, R., Jroundi, F., Geffers, R., Jarek, M., Link, A., Vilchez-Vargas, R., Merroun, M.L., 2022. Genetic mechanisms for Se(VI) reduction and synthesis of trigonal 1-D nanostructures in *Stenotrophomonas bentonitica*: perspectives in eco-friendly nano-material production and bioremediation. *Science of the Total Environment* in press.
- Rallakis, D., Michels, R., Brouand, M., Parize, O., Cathelineau, M., 2019. The role of organic matter on uranium precipitation in zoovch ovoos Mongolia. *Minerals* 9, 310. <https://doi.org/10.3390/min9050310>.
- Rallakis, D., Michels, R., Cathelineau, M., Parize, O., Brouand, M., 2021. Conditions for uranium biomineralization during the formation of the Zoovch Ovoos roll-front-type uranium deposit in East Gobi Basin Mongolia. *Ore Geol. Rev.* 138, 104351. <https://doi.org/10.1016/j.oregeorev.2021.104351>.
- Reiller, P., Descostes, M., 2020. Development and application of the thermodynamic database PRODATA, dedicated to the monitoring of mining activities from exploration to remediation. *Chemosphere* 251, 126301.
- Rexer, H.U., Schäberle, T., Wohlleben, W., Engels, A., 2006. Investigation of the functional properties and regulation of three glutamine synthetase-like genes in *Streptomyces coelicolor* A3(2). *Arch. Microbiol.* 186, 447–458. <https://doi.org/10.1007/s00203-006-0159-8>.
- Reynolds, R.L., Goldhaber, M.B., 1983. Iron disulfide minerals and the genesis of roll-type uranium deposits. *Econ. Geol.* 78, 105–120. <https://doi.org/10.2113/gsecongeo.78.1.105>.
- Rivett, M.O., Buss, S.R., Morgan, P., Smith, J.W.N., Bemment, C.D., 2008. Nitrate attenuation in groundwater: a review of biogeochemical controlling processes. *Water Res.* 42, 4215–4232. <https://doi.org/10.1016/j.watres.2008.07.020>.
- Robin, V., Beaufort, D., Tertre, E., Reinholdt, M., Fromaget, M., Forestier, S., de Boissezon, H., Descostes, M., 2020. Fate of dioctahedral smectites in uranium roll front deposits exploited by acidic in situ recovery (ISR) solutions. *Appl. Clay Sci.* 187, 105484. <https://doi.org/10.1016/j.clay.2020.105484>.
- Ruiz, O., Thomson, B., Cerrato, J.M., Rodriguez-Freire, L., 2019. Groundwater restoration following in-situ recovery (ISR) mining of uranium. *Appl. Geochem.* 109, 104418. <https://doi.org/10.1016/j.apgeochem.2019.104418>.
- Safonov, A.V., Babich, T.L., Sokolova, D.S., Grouzdev, D.S., Tourova, T.P., Poltarau, A.B., Zakharova, E.V., Merkel, A.Y., Novikov, A.P., Nazina, T.N., 2018. Microbial community and in situ bioremediation of groundwater by nitrate removal in the zone of a radioactive waste surface repository. *Front. Microbiol.* 9. <https://doi.org/10.3389/fmicb.2018.01985>.
- Sapsford, D., Cleall, P., Harbottle, M., 2017. In situ resource recovery from waste repositories: exploring the potential for mobilization and capture of metals from anthropogenic ores. *J. Sustain. Metall.* 3, 375–392. <https://doi.org/10.1007/s40831-016-0102-4>.
- Schmieder, R., Lim, Y.W., Edwards, R., 2012. Identification and removal of ribosomal RNA sequences from metatranscriptomes. *Bioinformatics* 28, 433–435. <https://doi.org/10.1093/bioinformatics/btr669>.
- Schneider, D., Schmidt, C.L., 2005. Multiple rieske proteins in prokaryotes: where and why? *Biochim. Biophys. Acta BBA - Bioenerg.* 1710, 1–12. <https://doi.org/10.1016/j.bbabi.2005.09.003>.
- Seaver, L.C., Imlay, J.A., 2001. Alkyl hydroperoxide reductase is the primary scavenger of endogenous hydrogen peroxide in *Escherichia coli*. *J. Bacteriol.* 183, 7173–7181. <https://doi.org/10.1128/JB.183.24.7173-7181.2001>.
- Seidler, A., Jaschkowitz, K., Wollenberg, M., 2001. Incorporation of iron-Sulphur clusters in membrane-bound proteins. *Biochem. Soc. Trans.* 29, 418–421. <https://doi.org/10.1042/bst0290418>.
- Sennhauser, G., Amstutz, P., Briand, C., Storchenegger, O., Grütter, M.G., 2006. Drug export pathway of multidrug exporter AcrB revealed by DARPin inhibitors. *PLoS Biol.* 5, e7. <https://doi.org/10.1371/journal.pbio.0050007>.
- Seredkin, M., Zabolotsky, A., Jeffress, G., 2016. In situ recovery, an alternative to conventional methods of mining: exploration, resource estimation, environmental issues, project evaluation and economics. *Ore Geol. Rev.* 79, 500–514. <https://doi.org/10.1016/j.oregeorev.2016.06.016>.
- Sharma, P.K., Sharma, V., Sharma, S., Bhatia, G., Singh, K., Sharma, R., 2019. Comparative metatranscriptome analysis revealed broad response of microbial communities in two soil types, agriculture versus organic soil. *J. Genet. Eng. Biotechnol.* 17, 6. <https://doi.org/10.1186/s43141-019-0006-3>.
- Sone, Y., Nakamura, R., Pan-Hou, H., Itoh, T., Kiyono, M., 2013. Role of MerC, MerE, MerF, MerT, and/or MerP in resistance to mercurials and the transport of mercurials in *Escherichia coli*. *Biol. Pharm. Bull.* 36, 1835–1841. <https://doi.org/10.1248/bpb.b13-00554>.
- Stolz, J.F., Basu, P., Oremland, R.S., 2002. Microbial transformation of elements: the case of arsenic and selenium. *Int. Microbiol.* 5, 201–207. <https://doi.org/10.1007/s10123-002-0091-y>.
- Sun, W., Sun, X., Li, B., Xu, R., Young, L.Y., Dong, Y., Zhang, M., Kong, T., Xiao, E., Wang, Q., 2020. Bacterial response to sharp geochemical gradients caused by acid mine drainage intrusion in a terrace: relevance of C, N, and S cycling and metal resistance. *Environ. Int.* 138, 105601. <https://doi.org/10.1016/j.envint.2020.105601>.
- Sun, W., Xiao, E., Häggblom, M., Krumins, V., Dong, Y., Sun, X., Li, F., Wang, Q., Li, B., Yan, B., 2018. Bacterial survival strategies in an alkaline tailing site and the physiological mechanisms of dominant phylotypes as revealed by metagenomic analyses. *Environ. Sci. Technol.* 52, 13370–13380. <https://doi.org/10.1021/acs.est.8b03853>.
- Supek, F., Bošnjak, M., Škunca, N., Šmuc, T., 2011. REVIGO summarizes and visualizes long lists of gene ontology terms. *PLOS ONE* 6, e21800. <https://doi.org/10.1371/journal.pone.0021800>.
- Vander Heiden, J.A., Yaari, G., Uduman, M., Stern, J.N.H., O'Connor, K.C., Hafner, D.A., Vigneault, F., Kleinstein, S.H., 2014. pRESTO: a toolkit for processing high-throughput sequencing raw reads of lymphocyte receptor repertoires. *Bioinformatics* 30, 1930–1932. <https://doi.org/10.1093/bioinformatics/btu138>.
- Vavourakis, C.D., Mehrshad, M., Balkema, C., van Hall, R., Andrei, A.-Ş., Ghai, R., Sorokin, D.Y., Muiyzer, G., 2019. Metagenomes and metatranscriptomes shed new light on the microbial-mediated sulfur cycle in a siberian soda lake. *BMC Biol.* 17, 69. <https://doi.org/10.1186/s12915-019-0688-7>.
- Wang, B., Weng, J., Fan, K., Wang, W., 2011. Elastic network model-based normal mode analysis reveals the conformational couplings in the tripartite AcrAB-TolC multidrug efflux complex. *Proteins Struct. Funct. Bioinforma.* 79, 2936–2945. <https://doi.org/10.1002/prot.23143>.
- Wersin, P., Hochella, M.F., Persson, P., Redden, G., Leckie, J.O., Harris, D.W., 1994. Interaction between aqueous uranium (VI) and sulfide minerals: spectroscopic evidence for sorption and reduction. *Geochim. Cosmochim. Acta* 58, 2829–2843. [https://doi.org/10.1016/0016-7037\(94\)90117-1](https://doi.org/10.1016/0016-7037(94)90117-1).
- Wood, D.E., Salzberg, S.L., 2014. Kraken: ultrafast metagenomic sequence classification using exact alignments. *Genome Biol.* 15, R46. <https://doi.org/10.1186/gb-2014-15-3-r46>.
- Yabusaki, S.B., 2014. Assessing the potential for bioremediation of uranium in situ recovery sites, Technical report NUREG/CR-7167. Technical report NUREG/CR-7167. United States Nuclear Regulatory Commission. Office of Nuclear Regulatory Research, Washington, DC.
- Yan, C., Wang, F., Geng, H., Liu, H., Pu, S., Tian, Z., Chen, H., Zhou, B., Yuan, R., Yao, J., 2020. Integrating high-throughput sequencing and metagenome analysis to reveal the characteristic and resistance mechanism of microbial community in metal contaminated sediments. *Sci. Total Environ.* 707, 136116. <https://doi.org/10.1016/j.scitotenv.2019.136116>.
- Yang, J., Pan, X., Zhao, C., Mou, S., Achal, V., Al-Misned, F.A., Mortuza, M.G., Gadd, G.M., 2016. Bioimmobilization of heavy metals in acidic copper mine tailings soil. *Geomicrobiol J.* 33, 261–266. <https://doi.org/10.1080/01490451.2015.1068889>.
- Zhao, L., Deng, J., Xu, Y., Zhang, C., 2018. Mineral alteration and pore-plugging caused by acid in situ leaching: a case study of the wuyier uranium deposit, XinjiangNW China. *Arab. J. Geosci.* 11. <https://doi.org/10.1007/s12517-018-4064-7>.